Advances in Colloid and Interface Science 286 (2020) 102297

Contents lists available at ScienceDirect

Advances in Colloid and Interface Science

journal homepage: www.elsevier.com/locate/cis

Historical Perspective

Detection of food spoilage and adulteration by novel nanomaterial-based sensors

Zahra Mohammadi, Seid Mahdi Jafari *

Department of Food Materials and Process Design Engineering, Gorgan University of Agricultural Sciences and Natural Resources, Gorgan, Iran

ARTICLE INFO

Article history:
13 October 2020
Available online 24 October 2020

Keywords:
Nanosensors
Monitoring
Food fraud
Food safety
Adulteration
Spoilage

ABSTRACT

Food industry is always looking for more innovative and accurate ways to monitor the food safety and quality control of final products. Current detection techniques of analytes are costly and time-consuming, and occasionally require professional experts and specialized tools. The usage of nanomaterials in sensory systems has eliminated not only these drawbacks but also has advantages such as higher sensitivity and selectivity. This article first presents a general overview of the current studies conducted on the detection of spoilage and adulteration in foods from 2015 to 2020. Then, the sensory properties of nanomaterials including metal and magnetic nanoparticles, carbon nanostructures (nanotubes, graphene and its derivatives, and nanofibers), nanowires, and electrospun nanofibers are presented. The latest investigations and advancements in the application of nanomaterial-based sensors in detecting spoilage (food spoilage pathogens, toxins, pH changes, and gases) and adulterants (food additives, glucose, melamine, and urea) have also been discussed in the following sections. To conclude, these sensors can be applied in the smart packaging of food products to meet the demand of consumers in the new era.

Contents

* Corresponding author.
E-mail address: smjafari@gau.ac.ir (S.M. Jafari).

https://doi.org/10.1016/j.cis.2020.102297
0001-8686/

1. Introduction

Food security and safety are recognized as one of the most critical human priorities since the world's population is continuously growing. The industrialization of food and agriculture is a strategy that guarantees continued access to food. However, microbial, chemical, and physical contaminants from harvesting to storage and marketing of products affect food quality and safety. On the other hand, profiteers have always posed a serious threat to public health since they are looking for different tactics to reduce production costs and achieve higher profits by adulteration. Unfortunately, millions of people die every year from diseases caused by unhealthy and adulterated foods [1]. Long-term analysis from several hours to several days and various pre-treatment stages are the main drawbacks of the current methods for assessing food safety such as cell culture, microbiological techniques [2,3], and chemical assays [4]. Also, these techniques are expensive and insensitive or demand considerable scientific expertise. Hence novel methods of the monitoring of food quality and safety not only reinforce the capacity to control the food cycle from farm to table but also provide efficient surveillance systems to ensure human health and consumer confidence [5,6].

Nanotechnology has presented innovative solutions to meet the challenges of many industries, including the food and pharmaceutical industry. Nanostructured materials can be classified into four different groups depending on how many dimensions they have on the nanoscale (1–100 nm): (i) zero dimensions (nanoparticles, nanoclusters, and quantum dots); (ii) one dimension (nanorods, nanotubes, and nanofibers); (iii) two dimensions (nano-thin films); and (iv) three dimensions (nanocomposites and bulk nanomaterials); these nanomaterials can be produced by top-down or bottom-up methods [7]. Nanostructures exhibit unique properties and thus open a new window of opportunity for the creation of innovative and high-performance materials that have significant effects on the control of food safety and quality. In this regard, nanomaterials have been used to achieve more accurate, rapid, and selective sensors and biosensors [8–10]. These nanosensors can be utilized for monitoring the food processes [11], detecting the contamination and adulteration at source and during the production chain [12,13], and the product spoilage [14–17]. In this regard, a recently published chapter gives more information about the detection methods of foodborne pathogens, including the nanosensors, and their advantages and disadvantages [18].

The main purpose of this paper is to present a focused review of the investigations published in the field of nanosensors for the detection of adulteration and spoilage in food products during the last few years; we will not cover earlier published articles unless they were considered necessary. After a general overview and evaluation of trends in this field, the fundamental concepts of nanosensors and the properties of nanostructures mostly used in nanosensor construction will be presented. Finally, recent advances in the detection of spoilage and adulteration in food products by nanomaterial-based sensors will be discussed. Although there have been some previous reviews on the application of nanosensors for the detection of pathogens and microbial toxins [19–23], there are very limited review papers on the application of nanosensors for the diagnosis of food spoilage and adulteration. To the best of our knowledge, this is one of the first attempts in this important field.

2. A general overview of nanosensors

Nanosensors are highly advanced yet precise and sensitive systems capable of detecting one or more specific physical or chemical phenomena based on a particular signal. These sensors operate on a nanometer scale and even react to the presence of several atoms in a single gas, which offer significant enhancements in speed, selectivity, and sensitivity in comparison with conventional chemical and biological techniques. Chemical nanosensors usually detect the presence or absence of an analyte or its concentration. Moreover, the nanosensors which their recognizing part has a biological nature (such as DNA strands, antibodies, enzymes) are known as nanobiosensors. Also, the application of different nanomaterials in the construction of biosensors can promote their sensitivity and other properties [19].

In general, nanosensors are fabricated by combining a receptor and a transducer. Any organic or inorganic substance can play the role of receptor and interact with the analyte or its derivatives, as shown in Fig. 1. However, the role of the transducer is to convert the response to the determinable signal [24]. This signal comes in various forms, including electrical [25], electrochemical [26], and optical [27] signals. Nanosensors are evaluated with several main characteristics. “Selectivity” is a vital characteristic of the sensors that indicates to what extent the system can separate the analyte from the other materials in the sample. In other words, the higher selective sensors can detect and measure the analyte with the least disturbance from the other materials within the sample. The next important characteristic is “sensitivity”. High sensitivity means that with the slightest variations in the analyte concentration, a significant change in the sensor output signal is observed. “Repeatability” is another essential characteristic defined by the word precision. The high precision indicates that the results of the repeated measurements are close together. Accuracy indicates that the measurement results are close to the actual value [28].

A literature review using the *Web of Science* database showed that from 2015 to 2020 (April 7), published articles on the nanosensors in various sciences such as materials science, analytical chemistry, nanotechnology, applied physics, electrochemistry, and optics have been increased substantially (55,380 in total), about 2.9% of which were conducted in the Food Science (1,960 articles). About 21.1% of Food Science nanosensor studies have focused on the detection of adulteration and spoilage in food products (414 articles) published mainly by researchers from China, India, USA, South Korea, Iran, Turkey, and Brazil, as shown in Fig. 2a. Moreover, the total number of citations of these publications in the recent five years has been 4,540 times (10.97 average citations *per* article), about 77% of them were between 2018 until 2020 (3480 citations), which is considerable. Expanding the number of articles published in the detection of adulterants and spoilage in foods, mostly in high-impact factor Journals prove the importance of this domain of research (Fig. 2b). The distribution of nanosensor applications in the detection of adulterants and spoilage species is given in Fig. 2c. Accordingly, around 70% of these studies were related to the detection of spoilage species, 44.4% of them focusing on the diagnosis of *Escherichia coli*, *Salmonella*, and *Staphylococcus aureus*, which is notable. Changes in pH value have been used to detect both spoilage and contamination of food products (7.7%). On the other hand, the most

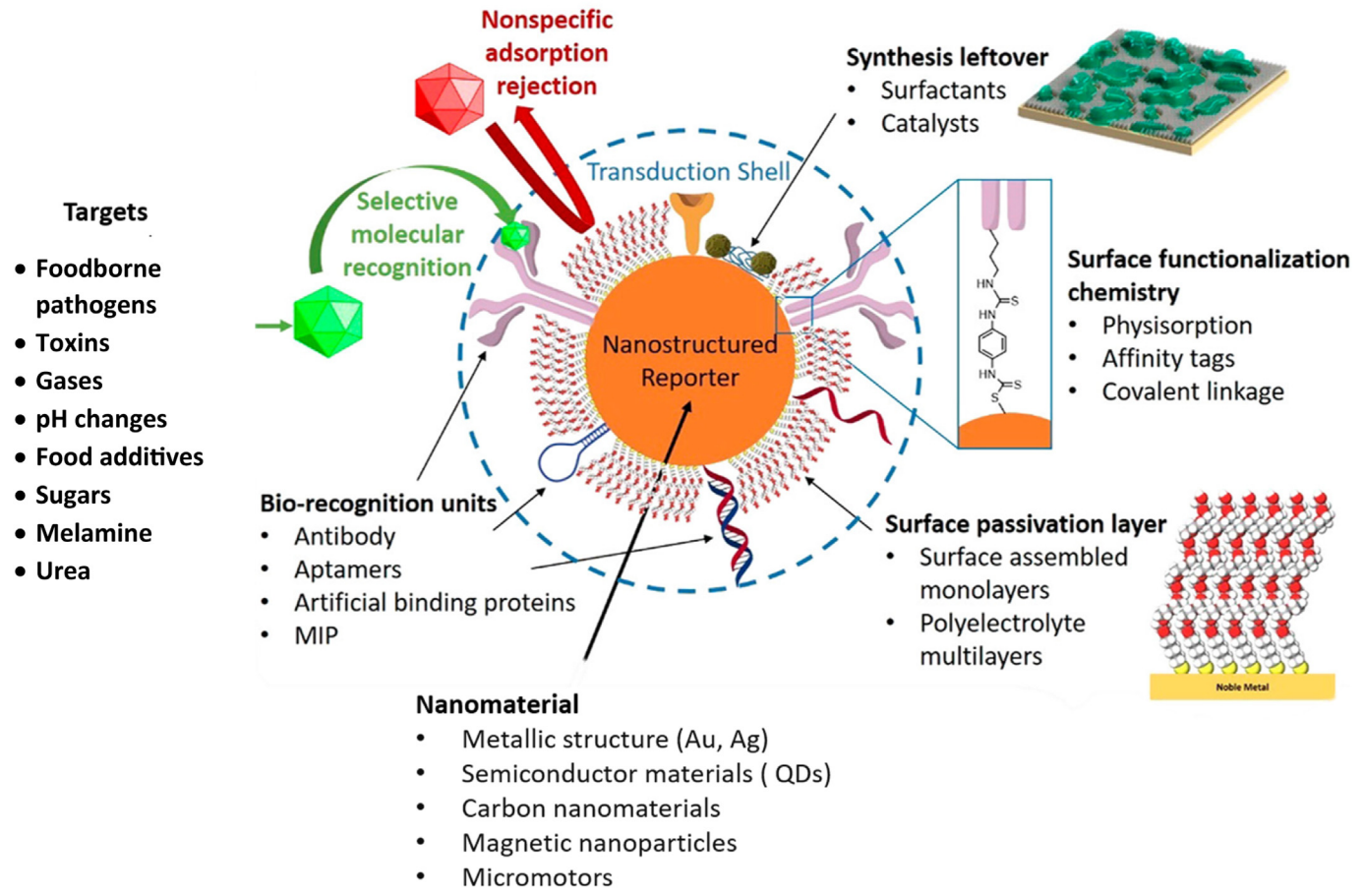

Fig. 1. Schematic of a nanobiosensor showing the recognition, reporting, and transducing elements. Adapted and reprinted with permission from [29].

adulterants that have been considered are dyes, glucose, and melamine (11.8%).

3. Sensory properties of nanostructures

Nanostructures mainly used for the construction of nanosensors include nanoparticles (metal, magnetic ones, quantum dots), carbon nanomaterials (nanotubes, graphene and its derivatives, and nanofibers), nanowires, and electrospun polymeric nanofibers. In general, the sensitivity and efficiency of sensors and biosensors are improved by employing these nanomaterials in construction. In the following sections, some properties of these nanomaterials related to the design of the nanosensors are presented, as summarized in Table 1.

3.1. Nanoparticles

Nanoparticles (NPs) are particles between 1 and 100 nm in diameter, the most important of which are metal, metal oxide, magnetic, quantum dots, semiconductor, and ceramic NPs. These NPs are found in various forms such as spheres, needles, rods, and plates. In general, the ratio of surface to volume and distance of energy level changes by varying the size of NPs. These two variables cause many of the NP properties to change. Although NPs play critical roles in various electrochemical procedures regarding their unique properties, the main performances of NPs can be generally classified as follows: (1) catalysis of electrochemical reactions; (2) increase in the electron transfer; (3) immobilization of biological molecules; and (4) labeling of biological molecules [30].

3.1.1. Metal nanoparticles

Metal NPs have investigated substantially amongst the researchers and the applied industries of Nanoscience and Technology [31]. Scientists have been researching metal NPs, also called colloidal metals or fine metal particles, for the past 150 years.

Generally, Localized Surface Plasmon Resonance (LSPR) is the cause of the optical properties of metal NPs, which is one of the distinctive properties of these particles from large-scale materials. When light hits metal surfaces, some light waves scatter along metal surfaces, creating surface plasmons (in fact, they give part of their energy to surface electrons and cause vibrations). When plasmons are produced in bulk metals, electrons can transfer freely in materials without any effect. In the NPs, the surface plasmon is confined to space, such that electrons in this small space oscillate in the same direction. This effect is called the LSPR. In most metals, the surface plasmon frequency is at the frequencies of ultraviolet (UV) light, so almost all visible light is reflected. Thus, the appearance of most metals is white and bright (perfectly reflecting visible light). The size and morphology of metal NPs and the dielectric properties of their surrounding environment significantly affect their surface plasmon properties. Metals such as gold and silver have a very strong visible plasmon resonance, while many other intermediate metals have only a weak and broad absorption band in the UV region. It is recalled that metals in the form of NPs have a much higher surface area and thus have a higher surface plasmon activity. On the other hand, the dielectric properties of an environment can be significantly altered by the presence of a chemical agent (analyte). These two points lead to a new concept: surface plasmons of metal NPs can be used to detect various types of molecules and proteins present in the environment. In other words, this concept has brought about widespread applications to surface plasmon resonance phenomena,

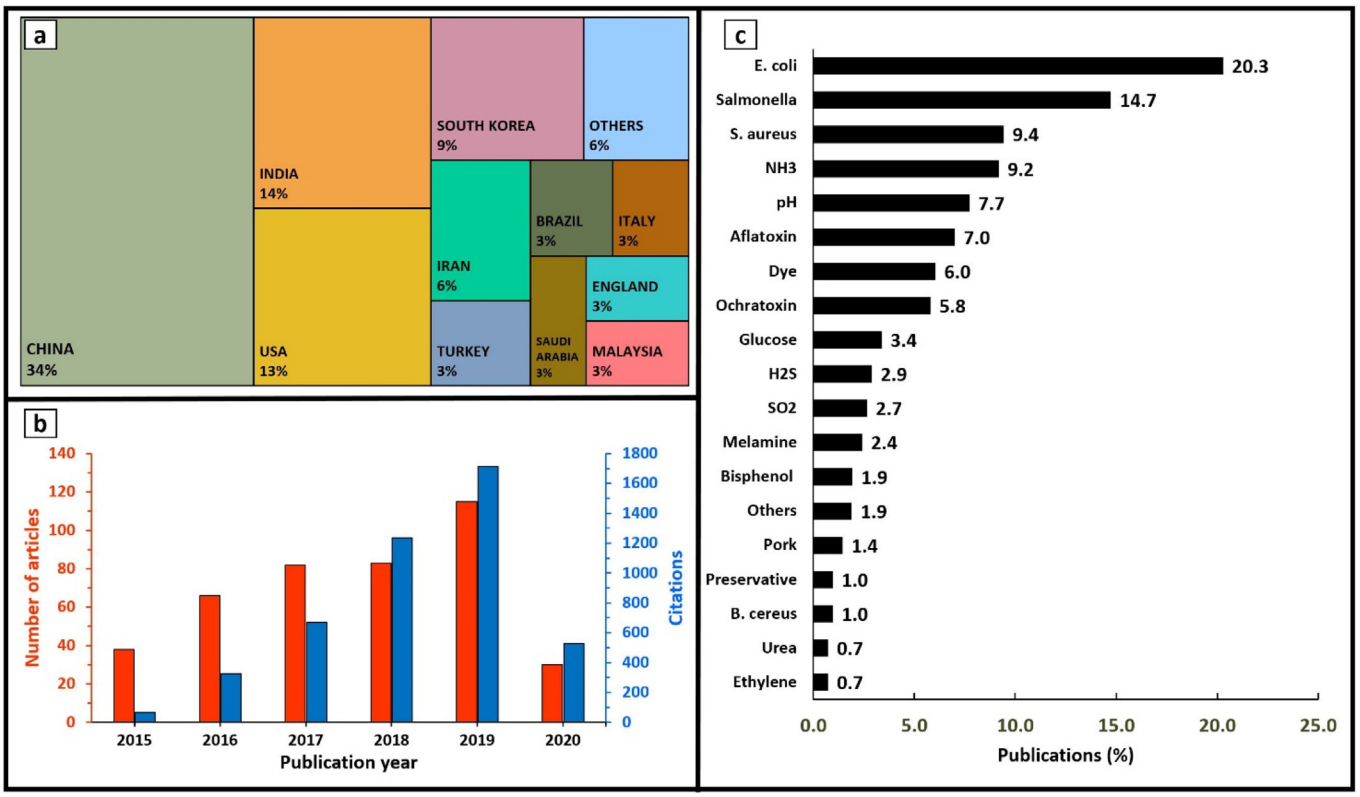

Fig. 2. Overview of the publications focusing on detection of spoilage and adulterants in foods during 2015–2020 (April 7) in relevance to (a) countries, (b) publication year, and (c) analytes. Source: *Web of Science* database using "nano* AND sensor AND food AND (spoilage OR adulteration)" (or derivative words), and the specific substances as keywords.

some of which are: enhanced surface spectroscopy, biological, chemical, and molecular sensors [32].

On the other aspect, two types of surface plasmons are used to produce plasmon-based sensors: Propagating Surface Plasmon Resonance (PSPR), and LSPR. In the PSPR method, the fading electromagnetic waves are surrounded by the metal-dielectric contact surface, while in the LSPR, the electromagnetic waves are confined to the metal nanostructures. Sensors made by both methods are sensitive to local refractive index variations so that by binding the target particle onto the surface, the refractive index variations can be detectable. In this approach, the particle-to-surface bonding is directly converted to a signal and does not require labeling; whereas, in conventional optical sensors, chromophores and fluorophores are needed. Due to the high surface sensitivity, label-free, and real-time measurement of events, the number of PSPR-based sensors is increasing and researchers are developing them for the identification of molecular binding through binding sites. The LSPR-based sensors are easily adjustable and modifiable so that the shape, size, and chemical composition of NPs as the primary sensing elements can be tuned. This advantage, along with the other benefits of PSPR, will help researchers. LSPR-based nanosensors are used to identify chemicals and biomaterials. In most cases, when a specific bond is created between the target analytes and the surface, the plasmonic band is displaced, which is used as a signal for detection [33].

Metal NPs such as gold (Au), and silver (Ag) NPs and metal oxide NPs such as titanium dioxide (TiO_2), zinc oxide (ZnO), and silica (SiO_2) NPs are used in many high-tech applications including sensors, adsorbent materials, drug delivery systems, and antimicrobial materials, among many others [34–37].

3.1.2. Magnetic nanoparticles

Magnetic NPs (MNPs) are referred to as particles of an independent nature with a maximum size of 100 nm and containing magnetic elements. These particles have unique physical and chemical properties that are dramatically different from the bulk state of the material [38]. In nature, three elements of iron, nickel, and cobalt, and other elements combined with them have magnetic properties. One limitation is that only certain compounds can have magnetic properties. One of the interesting and very useful properties of nano-dimensional properties is that many materials without magnetic properties in ordinary dimensions can have magnetic properties in the nanotechnology domain. For instance, aluminum oxide and Au NPs can be some examples. This eliminates the limitations mentioned above and, given the wide application of magnetic materials, new materials with improved properties can be produced. For instance, the magnetic properties of some NPs are used in medicine for drug delivery. The reason for no magnetic properties of some materials in ordinary dimensions is the large increase in their surface area and the formation of broken bonds on their surface. When a bond is formed, two electrons are in an orbital in opposite directions, neutralizing each other's magnetic fields. Though, the incomplete or broken bond implies that there is a single electron in the orbital and the other electron does not neutralize its magnetic field. At the nanoscale, most materials have magnetic properties since many atoms and the broken bonds are on their surface [7].

Among NPs, MNPs have attracted the most attention due to their easy separation with an external magnetic field and their high capacity for use in a variety of areas such as advanced materials, medicine, diagnostic techniques, energy, and food [39–42]. Furthermore, MNPs attached to diagnostic biomolecules can be used to magnetically separate and empower samples for detection [43]. In the food application of MNPs, it is crucial to examine the safety or toxicity of these particles. Hence among the types of MNPs, iron oxide (IO) NPs, especially superparamagnetic Fe_3O_4 (magnetite) NPs, have been the most commonly used in food due to their lack of toxicity, excellent compatibility, and lack of preservation of residual magnetism after removal of the external magnetic field. Also, by modifying the surface, IO NPs can be functionalized with special groups such as NH_2, -COOH, -OH to be suitable

Table 1
Summary of sensory properties of some nanomaterials used in the construction of nanosensors.

Nanomaterials	Type	Example material	Sensory properties	Description
Nanoparticles	Metal NPs	Pure metals (e.g., Au, Ag, Pt, Ti, Zn, Fe, and Tl) or their compounds (e.g., oxides, hydroxides, sulfides, phosphates, fluorides, and chlorides)	Optical properties due to the LSPR and PSPR	Au and Ag NPs have a powerful visible plasmon resonance, while many other intermediate metals have only a weak and broad absorption band in the UV region.
	Magnetic NPs	Magnetic material, often Fe, Ni, and Co	Easy separation with an external magnetic field/Empowering samples for detection through bioconjugation and immobilization	IO NPs, especially superparamagnetic Fe_3O_4 (magnetite) NPs, have been the most commonly used in food due to their lack of toxicity, excellent compatibility, and lack of preservation of residual magnetism after removal of the external magnetic field.
	Quantum dots	Semiconductors, metals, magnetic materials	Fluorescent behavior	The emission of QDs is usually in the range of 450–850 nm. Stokes' Shift improves their tracking sensitivity.
Carbon nanomaterials	CNTs	Carbon	Change in their conductivity and semiconductor based on their geometric shape/unique ballistic conduction/high thermal conductivity/distinctive electrical and mechanical properties/emission and absorption of light/high surface density/high tensile strength	SWCNTs: excellent mechanical and electrical properties/production, along with stabilizing their properties, is expensive and very difficult. MWCNTs: easier manufacturing, availability, and commerciality/lower strength compared to single-walled type.
	Graphene	Carbon	Quantum Hall effect/high electron mobility at room temperature/ability to absorb 2.3% light/exceptional thermal conductivity/high mechanical strength/large specific surface area	GO, rGO, and GQDs are the main representatives of this group.
	CNFs	Carbon	Very conductive/their entire surface can be activated	One of the significant limitations of CNFs is low electrical conductivity. Methods that can be used to increase their electrical conductivity include coatings with metals, metal oxides, CNTs, and graphene.
Nanowires	Metal NWs	Metals, semiconductors, oxides, sulphides, nitrides	Performing well in the process of electron transfer and light activities	Using NWs as electronic channels to detect based on the direct recording of electrical conduction
Nanofibers	ENFs	Natural polymers, polymer blends, nanoparticle- or drug-impregnated polymers, and ceramic precursors	High surface area relative to unit volume/high porosity/strong mechanical properties/high axial tensile with high flexibility/low weight	Their morphology can be adjusted/their surface structure can be modified to create different properties/controlling the secondary structures to provide core-shell structures, hollow or porous internal structures

NPs = nanoparticles; LSPR = localized surface plasmon resonance; PSPR = propagating surface plasmon resonance; Au = gold; Ag = silver; Pt = platinum; Ti = titanium; Zn = zinc; Fe = iron; Tl = thallium; Ni = nickel; Co = cobalt; UV = ultra violet; IO = iron oxide; CNTs = carbon nanotubes; SWCNTs = single-walled CNTs; MWCNTs = multi-walled CNTs; GO = graphene oxide; rGO = reduced GO; GQD = graphene quantum dots; CNFs = carbon nanofibers; ENFs = electrospun nanofibers.

for further binding to molecules with various applications [44]. Switchable systems that can be used as hydrogen peroxide biosensors are also made with MNPs [45]. In addition, magnetic cell separation techniques apply magnetic field gradients for separation and manipulation, and magnetically labeled cells [46]. Further, magnetic immunoassay techniques have also been developed in which the magnetic field generated with magnetically labeled targets is detected directly with a magnetometer [47,48]. In this technique, in order to quickly detect biological targets, supermagnetic NPs and a microscope based on high temperature transfer of direct current of a superconducting quantum interference device are used. Also, through chemical functionalization of magnetic nanomaterials, it is possible to bioconjugate these nanoparticles to the desired analyte, which has been used in sensory systems. Electrochemical and optical sensors have been produced to detect hemoglobin, peroxide, *Listeria*, *E. coli*, and lysozyme by this method [49].

3.1.3. Quantum dots

In the last decades, numerous investigations have been prepared on fluorescent NPs (FNPs), including quantum dots (QDs). Semiconductor QDs (SQDs), carbon QDs (CQDs), and graphene QDs (GQDs) are fluorescent dots. The fluorescent behavior of these NPs is altered by interactions with molecules and surrounding materials. There are various studies that show this property of QDs can be adopted to detect and measure particular analyte [50–54].

SQDs are nanocrystals that consist of a semiconductor core and another semiconductor as a shell with a larger energy gap. They were first used in 1982 to study surface kinetics. The core of SQDs usually consists of elements of groups II and VI of the periodic table, or groups III and V, while the shell is composed of materials with more energy gaps. SQDs are usually 1 to 10 nanometers in size, allowing them to interact one by one with biological molecules such as proteins with a size range of 1 to 20 nanometers [55]. Due to the special electrical properties and the type of response that results from the interaction of a species with quantum dots in the fluorescence emission of these nanoparticles, the application of quantum dots to develop various sensors has become a key factor in recent years.

QDs are inorganic fluorophores that have a size-tunable emission, meaning that the wavelength of their emission increases with increasing size. Strong optical absorption, bright emission, narrow and symmetrical emission spectrum, and high optical stability are other properties. QDs also maintain their emission intensity after binding to biological molecules. The emission of QDs is usually in the range of 450 to 850 nm. If the QDs are single-core, the quantum efficiency is 10%, but with the shell, this efficiency increases to 80%. The large gap between the excitation and emission spectrum (Stokes' Shift) improves their tracking sensitivity. The unique optical properties of QDs and their surface properties provide biological stability and various bindings, making these nanoparticles a fluorescent indicator for biological applications compared to classic organic fluorescents [56].

QDs are derived from the name of the quantum confinement effect, which is the basis of their function. This effect is observed in the optical properties of semiconductor materials less than 10 to 20 nanometers. Moreover, the relationship between the size of the QDs and the wavelength of their emission is related to this effect. When the QDs are smaller than the exciton Bohr radius, the energy level for a photon is quantized, and there is a direct relationship between the size of the

QDs and the quantum energy values. When QDs are exposed to light, photons absorb energy with higher energy than the gap, which excites the electrons. Therefore, the possibility of energy absorption at higher wavelengths leads to a wider stimulus spectrum. Therefore, the possibility of energy absorption at higher wavelengths leads to a wider stimulus spectrum. When excited electrons return to lower energy levels, a narrow and symmetrical emission spectrum occurs. The duration of the molecules remaining in the excited state is almost long (10 to 40 nanoseconds), making the fluorescence stable and strong [57].

3.2. Carbon nanomaterials

Among the various nanostructures, carbon nanomaterials have received much attention because of their excellent thermal stability, electrical conductivity, and high contact surfaces [58]. Carbon compounds have been recognized as functional electron transfer intermediates due to their properties such as low field emission, large potential windows, chemical inertness, and low cost [59]. Since carbon is entirely inert, the deposition of nano-crystalline metals on the carbon nanotubes (CNTs) and carbon nanofibers (CNFs) provides a unique opportunity to fabricate new types of composite electrode structures with high stability and electrical conductivity [60]. Various carbon structures such as graphite, glassy carbon, nanofibers, nanotubes, non-crystalline powders, and diamond have been used as electrodes [61,62]. Recently, graphene, as one of the new carbon allotropes, is surpassing CNTs in the production of sensors. One of the most major reasons for the development of carbon nanomaterial-based sensors is that these materials have considerable stability in addition to having a regular nanoscale structure. Hence, they are stable even when not functional [63].

3.2.1. Carbon nanotubes

Nanotubes are one of the candidates for constructing chemical and mechanical nanosensors. CNTs were discovered in 1991 by Japanese scientists which are graphite tubes. Tiny size, changes in their conductivity and semiconductors based on their geometric shape, unique ballistic conduction, high thermal conductivity, distinctive electrical and mechanical properties, high Young modulus, emission and absorption of light, high surface density, and high tensile strength are some of the significant attributes of CNTs that have led to their applications in various industries [64].

The nanotubes are divided into two groups of single-walled (SWCNTs) and multi-walled (MWCNTs). SWCNTs consist of only one single layer of graphene cylinders (a sheet of regular hexagons); whereas in MWCNTs, many graphene sheets (approximately 50) are piped. The reason for interest in SWCNTs is due to their special characteristics, such as their conductive or semiconductor ability and their excellent mechanical and electrical properties. On the other hand, the production of SWCNTs, along with stabilizing their properties is costly and very difficult. Unlike SWCNTs, easier manufacturing, availability, and commerciality of MWCNTs have led to further advances in this area. These nanomaterials also have disadvantages, including a lower strength compared to single-walled types. However, since the employ of CNTs is mostly due to their thermal and electrical properties, the utilization of MWCNTs is more widespread than SWCNTs [65].

CNTs have created an important attraction in nanosensors and nanoelectronic devices due to their unique properties. These properties are highly dependent on physical appearance, including diameter, length, catalyst presence, and chirality. For instance, SWCNTs can be metallic or semiconductor depending on the natural distance between the bond and torsion [66]. SWCNTs are used in field-effect devices. Plus, semiconductor CNTs reveal outstanding conductivity changes in response to the physical adsorption of various gases. Thus, SWCNTs-based nanosensors can be fabricated founded on the field-effect transistor design, in which the adsorbed molecules that regulate the nanotube conductivity replace the valve in the closed position [67]. Semiconductor SWCNT is the preferred nanomaterial for sensors since its mobility is high and all its atoms are on the surface. These sensors have several advantages in detecting and identifying biological species: first, they form the conductor channel in the transistor configuration. Second, nanotubes are usually placed on the surface and are in direct contact with the environment. The geometric shape of this device contrasts with the metal oxide semiconductor field-effect transistors, where the conducting channel is covered in bulk material and a vacant layer is formed. Finally, all the current flows on the surface of the CNTs. All of these remarkable features lead to a field-effect transistor device that is extremely sensitive to minor changes in the environment [68–70]. The binding of biological molecules to these nanomaterials has also been investigated. Small proteins can be trapped by simple physical adsorption into the inner channel of opened nanotubes. Binding of small proteins to the outer surface of CNTs is also possible by hydrophobic and electrostatic interactions through covalent bonding or functionalization around the nanotubes with polymer coatings [71].

3.2.2. Graphene and its derivatives

Graphene is the name of one of the carbon nanostructures. In this material, atoms of carbon are formed in a single, flat layer in a two-dimensional hexagonal lattice structure with a carbon-carbon bond length of 0.142 nm. In this structure, carbon atoms have an sp^2 hybridization. These bonds and orbital arrangements are the causes of the extraordinary characteristics of this nanosheet, which will be mentioned below. It can also be assumed that each graphite-based material is composed of graphene, including dimensionless fullerenes, one-dimensional CNTs, and three-dimensional graphite, and despite its flexibility, it is harder than diamonds and conducts electricity faster than anything else at room temperature. Electrons in graphene behave like particles without mass, which leads to extraordinary properties such as the quantum Hall effect. Graphene has numerous other interesting properties, including high electron mobility at room temperature (250,000 cm^2/Vs) and the ability to absorb 2.3% light, exceptional thermal conductivity (5,000 W/mK), high mechanical strength (based on Yang module equal to 1 TP, which is 200 times higher than steel) and large specific surface area (2630 m^2/g, which is twice of single-layer CNTs) [72].

By reducing the dimensions of graphene to narrow chips with a width of 1 to 2 nm, a separate strip gap is created in graphene, which makes graphene quasi-conductive and produces potential applications in the construction of transistors [73]. Graphene oxide (GO), reduced graphene oxide (rGO), and graphene quantum dots (GQDs) are the main representatives of this group. GO is the most common graphene derivative produced during the oxidative reaction of graphite by Hummer's method. [74,75]. rGO can be gained by thermal and chemical reduction of GO [76]. On the other hand, 1 to 10 layers of graphene or reduced graphene form the structure of GQDs. The reason for using this nanomaterial in the design of biosensors is its low toxicity and desirable biocompatibility [77].

On account of the remarkable physical and electrochemical characteristics mentioned above, graphene has been extensively explored in the field of electroanalytical chemistry. In addition to the electrical conductance over the large surface of graphene, it also efficiently attaches onto the analyte molecules and transfers electron very fast, leading to a higher sensitivity of graphene-modified electrodes [78]. Diversity in graphene surface modification with chemical and biological functional groups such as amine, hydroxyl, sulfonate, and carboxyl causes different properties and behaviors [79]. Similarly, there are different techniques to improve the surface of graphene by employing nanomaterials and long-chain polymers. A wide range of analytes such as urea, glucose, hydrogen peroxide, cholesterol, and cancer cells, are detectable by graphene used in biosensors [80,81]. Graphene is also used to transfer electrons from oxidation and reduction centers in metalloproteins [82]. In optical applications, graphene has the ability to amplify Raman diffraction for organic molecules [83,84]. Graphene also suppresses a wide range of fluorescents [85,86]. Therefore, the application of

graphene and its derivatives in a wide range of sensors, including fluorescence sensors, surface-amplified Raman sensors, electrochemical sensors, sensors based on field-effect transistors, has been investigated.

3.2.3. Carbon nanofibers

CNFs are cylindrical nanostructures with different arrangements of graphene sheets. These clumps can be in the form of small graphene clumps in fluid systems with lattice surfaces or precise channels. Other structures are also seen as ribbon or herringbone, stacked cones, cups, plates, tubular, and no hollow core with many edge sites on their outer wall. Normally, their diameter is in nanoscale, while their length is micrometers. Vapor grown carbon fibers and their smaller counterparts, vapor grown CNFs, are in the category of short carbon fibers. CNFs have received a great deal of attention due to their excellent potential for improving thermal, electrical, frequency, and mechanical properties. These materials are widely used in various systems such as composites due to their exceptional properties and low cost [87].

In contrast to electrical properties, the mechanical strength of CNFs is similar to that of CNTs (although CNTs are very conductive). The main differentiation of CNFs from CNTs is the aggregation of graphene sheets in different shapes, which causes more defects on the outer wall of CNFs than CNTs [88]. Further defects at the edges can facilitate the electron transfer to the electroactive analytes. Moreover, CNFs are unique so that their entire surface can be activated. Because CNFs have a higher level of functionalization than CNTs, the ratio of the surface area of the active groups to the volume of these materials is more extensive than CNTs. These properties indicate that CNFs can operate as electrochemical signal transducers. All these unique characteristics of CNFs make them useful for the construction of a wide range of high-performance electrochemical sensors and biosensors.

These nanofibers have been used as a suitable substrate for the immobilization of a variety of enzymes, including oxidases, dehydrogenases, and other biomolecules for the production of biosensors, which are highly sensitive and maintain enzyme activity at their surface [60]. Mesoporous CNFs with a relatively high surface area (20–200 m^2/g) have been well defined as a tunable nanostructure. So these materials appear to be appropriate substitutes for activated carbon [89]. As mentioned, one of the major limitations and drawbacks of CNFs is their low electrical conductivity. Some methods that can be used to increase their electrical conductivity include coatings with metals, metal oxides, CNTs, and graphene [90].

3.3. Nanowires

Nanowires (NWs) are an essential and significant category of one-dimensional nanomaterials since they perform well in the process of electron transfer and light activities. These two properties play a vital and decisive role in the application of this category of nanostructures in the manufacture of nanometer instruments. Due to the large ratio of surface to volume and the capability of controlling the electrical conductivity due to quantum constraints, the electrical properties of these nanostructures are effectively changed by the least disturbance [91,92]. One of the advantages of one-dimensional systems compared to two-dimensional systems is that by connecting a molecule to their surface, a great change in their electrical properties happens. This property in one-dimensional nanostructures makes it possible to use them as electronic channels to detect based on the direct recording of electrical conduction. Similarly, if appropriate receptors are used, the interaction of the receptor located at the nanowire surface can be investigated simultaneously in response to a suitable substrate and thus measuring the substrate [93,94].

The main mechanism of the nanowire-based sensor is the field effect, which is converted to a field-effect transistor. This bottom-up method in bionanoelectronics has several diverse features: First, NWs are extremely sensitive to detect molecular interactions at their surface due to their long length-to-diameter ratio. Second, NWs provide electronically interchangeable properties of high-quality, signal-free, electrically readable sensor semiconductor nanowires. Third, NWs can be easily adjusted to smaller sizes below 100 nm, resulting in a higher density of a device on the chip. Therefore, it will be possible to construct a scaled-down tool to detect multiple samples in real time. Fourth, the unrestricted candida material as NWs provides researchers with more flexibility in selecting lightweight and useful materials for the sensor [95,96].

The construction of sensors based on metal NWs and arrays made of NWs began at the same time as the development of nanosystems and is still expanding. NW-based sensors are a large group of highly sensitive electrical sensors that can directly detect chemical and biological species. The size of nanostructures is the same as chemical and biological species [95]. As a result, due to the possibility of electrical communication between nanosystems and species, it is easy to detect them [97,98]. For example, a modified glass carbon electrode with Au NWs has been used to detect glutamate [99] and ZnO NWs have been prepared to construct lipid-based nanobiosensors [100].

3.4. Electrospun polymeric nanofibers

Nanofibers are nanoscale structures with unique characteristics such as a high surface area relative to unit volume, high porosity, strong mechanical properties, high axial tensile with high flexibility, low weight, and cost-effective compared to other nanostructures [101]. One of the interesting characteristics of nanofibers is that not only their morphology can be adjusted, but also their surface structure can be modified to create different properties. It is also possible to control the secondary structures of nanofibers to provide core-shell structures, and hollow or porous internal structures [102]. Conventional methods of nanofibers synthesis include wet spinning [103], dry spinning [104], melt spinning [105], sol-gel spinning [106], and electrospinning (ESP) [107].

ESP is a process for the production of thin and ultra-thin fibers, which was first invented in the year 1930. This unique, fast, simple, and low-priced technique is used to produce a variety of fibers, including polymer and ceramic fibers with diameters from 1 nm to several microns [108]. By definition, electrospun nanofibers (ENFs) refer to fibers <1000 nm in diameter. Typical ESP equipment consists of four main parts [109], as represented in Fig. 3: (i) a high voltage power supply; (ii) a syringe pump; (iii) a metallic spinneret; and (iv) a conductive collector.

The principle of this process is based on applying a very high voltage to a capillary needle and pulling the polymer solution out of it due to the electrostatic force generated by strong fields with a high potential difference (10–50 kV) [110], which transforms, accelerates and narrows the small volume of polymeric solution [111]. It becomes very thin in the form of fibers. In this process, a drop of solution is held by the surface tensile force on the tip of the nozzle and becomes heavily charged under the strong electric field between the nozzle and the collector. When the voltage reaches the threshold, the electrostatic force overcomes the surface tension of the solution and a cone is formed at the end of the drop, called the Taylor cone [112]. Then a very thin jet exits the Taylor cone. A very sharp decrease in diameter occurs during the transition from relatively large cone-shaped to thin fibers as a result of the bending instability of the jet that plots a turbulent path during rotation. Fibers with a diameter of 20–20000 nm can be produced in this method by choosing the appropriate polymer and solvent [16].

A comprehensive review paper investigated the methods and applications of ESP and ENFs [113]. By conjugating other nanomaterials such as graphene, CNTs, NPs to the surface of nanofibers, it is possible to fabricate multi-purpose nanostructures, produce novel ENFs, and improve sensing performance.

4. Nanosensors for detection of food spoilage

Every year, many people get foodborne diseases and in some cases die from eating food contaminated with bacteria, viruses, parasites, or

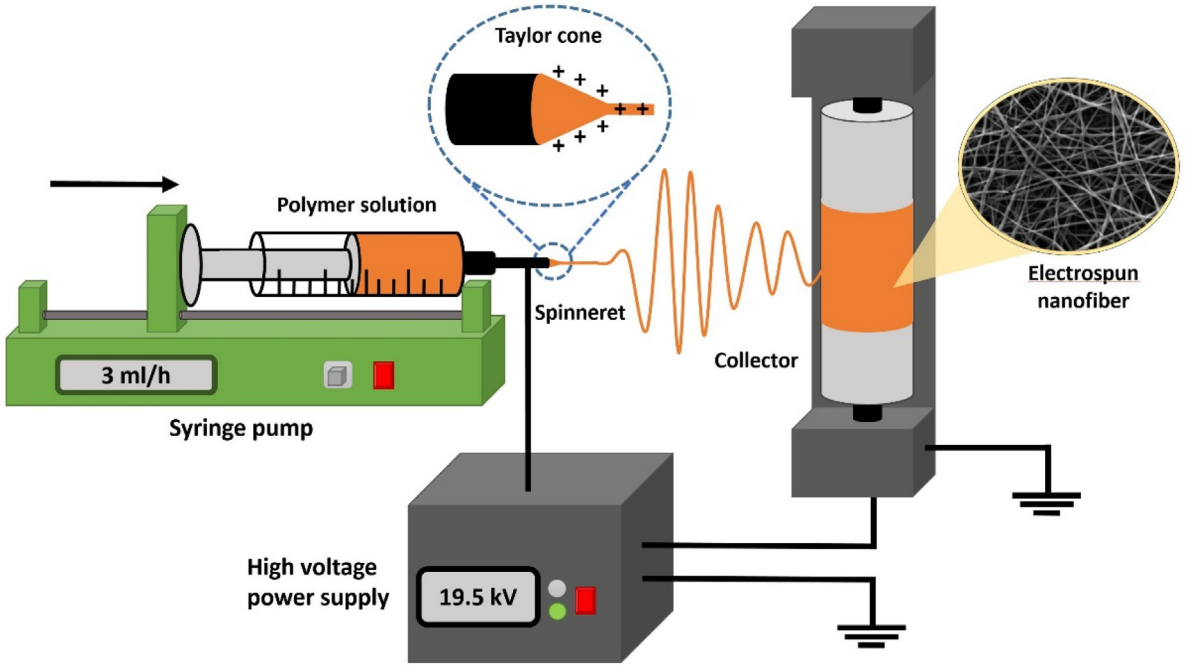

Fig. 3. Illustration of a typical electrospinning equipment setup for the production of nanofibers.

chemical substances. According to the World Health Organization, one in 10 people worldwide fall ill from contaminated food each year. So early detection of food spoilage has long been the focus of many researchers. The process of detecting spoilage alongside the chain of production, distribution, and consumption of perishable foods can lead to the construction of an intelligent system that monitors the quality of food in each part of the chain and warns if necessary. In general, the characterization of spoiled food is done by the detection of foodborne pathogens and non/toxic gases released from perishable foods, such as meat, fish, poultry, eggs, fruits, vegetables, and beverages. A summary of studies in this field is given in Table 2.

4.1. Detection of food spoilage pathogens

4.1.1. Escherichia coli and Salmonella

Enterobacteriaceae are a large group of Gram-negative, spore-free bacilli that normally live in the intestines of humans and animals. There are several genera in this family, the main of which are *E. coli* and *Salmonella*, which are the most significant causes of gastroenteritis and the microbial indices of water and food contamination. Their presence in drinking water and food indicates the contamination of these substances with other intestinal pathogens [119]. Research has shown that electrospun polyacrylic acid/polyvinyl alcohol (PAA/PVA) hydrogel nanofibers can be successfully used in the detection of *E. coli* in water as a sensing layer with a LOD of 20 CFU/mL. The reason for the high sensitivity of this biocompatible biosensor in this potentiometric method is the high sensitivity of these nanofibers to pH changes [114]. Another similar study using these pH-sensitive nanofibers was conducted to detect *E. coli* in a sample of orange juice with a LOD of 10^2 CFU/mL in less than 1 hour. The metabolic activity of *E. coli* toward sugar molecules and the production of acidic products such as lactates and acetates are the sensing mechanism of this portable sensor [115]. A case study was performed on *E. coli* and a threshold of 5 log CFU/mL bacteria was reported. This non-contact and wireless radio frequency identification (RFID) compatible sensor tag can be used for real-time quality monitoring of milk over the supply chain. In this method, cells that attach to conductive nanoparticles enable RF investigation [116]. In another exciting research, a combination of the isothermal recombinase polymerase amplification (RPA) with unmodified Au NPs were used to detect *Salmonella* in milk (with a LOD = 50 CFU), which was a more accurate, faster, and less expensive method than the national standard detection method (GB4789.4). This study was based on macromolecular adsorption of an enzyme, ssDNA, and unmodified Au NPs. This adsorption is affected by the subtle change of the solution due to amplification [120].

Yi, et al. [121] proposed an aptamer-based method for determining *Salmonella typhimurium*. In this method, carboxymethyl chitosan was loaded with improved amine aptamer against *S. typhimurium* and then adsorbed by electrostatic interaction on Au NPs to produce a composite that acted as a molecular diagnosis element, as shown in Fig. 4a. In another recent study, based on a specific matching between two aptamers embedded MNPs and cDNA-upconversion NPs (UCNPs), a fluorescence sensor was designed to screen *E. coli* (Fig. 4b). The fluorescence sensor achieved a lower limit of detection (LOD) (10 CFU/mL) in the linear range of 58–58 × 10^6 CFU/mL. One of the highlights of this work was the use of this sensor to detect *E. coli* in adulterated pork samples [117]. In another work, an electrochemical biosensor based on a Prussian blue-MWCNTs – Au NPs composites have been fabricated to identify *E. coli*. This PC based system was portable and can be employed for on-site monitoring using the cyclic voltammetry (CV) method to control food products as it is able to detect and measure the electrochemical activities of biomolecules [118]. Also, rGO-CNTs nanocomposites were used to prepare an accurate aptasensor to detect *S. typhimurium*. In this study, *Salmonella* bacterial cells were identified by combined amino-modified DNA aptamer to the nanocomposite without any pretreatment or DNA extraction steps. Under optimal experimental conditions, this label-free electrochemical sensor could detect *S. typhimurium* in a wide linear dynamic range from 10 to 10^8 CFU/mL with a 10 CFU/mL LOD [122]. Finally, Au NPs-assisted multiplex PCR assay was developed for the simultaneous detection of three pathogens, including *S. typhimurium*, *Listeria monocytogenes*, and *E. coli O157:H7*. The high performance of this color sensor made it possible to recommend it for the detection of pathogenic strains in food samples [119].

4.1.2. Staphylococcus aureus

Staphylococcus aureus is the most pathogenic species of the *Staphylococcus* genus which belongs to the *Staphylococcaceae* family and has

Table 2
Examples of nanomaterial-based sensors for the detection of spoilage in food analysis.

Target analyte	Nanomaterial	Method/technique	Linear range	Limit of detection	Recovery (%)	Food matrix	Reference
Escherichia coli	ENFs (PAA/PVA hydrogel)	LAPS	10^3–10^7 CFU/mL	20 CFU/mL	–	Water	[114]
	ENFs (PAA/PVA hydrogel)	LAPS	10^2–10^6 CFU/mL	10^2 CFU/mL	–	Orange juice	[115]
	d-Au NPs	RFID	–	5 log CFU/mL	–	Milk	[116]
	MNPs/cDNA- UCNPs	UCNPs coated with aptamer	58–58 × 10^6 CFU/mL	10 CFU/mL	97–107	Pork	[117]
	MWCNTs – Au NPs composite	CV	–	5 × 10^8 CFU/mL	–	–	[118]
	Au NPs	Colorimetric	–	50 pg/μL	–	–	[119]
Salmonella	Au NPs	RPA	–	50 CFU	–	Milk	[120]
	Au NPs	Colorimetric	10^2–10^9 CFU/mL	16 CFU/mL	92.4–97.2	Milk	[121]
	rGO-CNTs nanocomposite	DPV	10–10^8 CFU/mL	10 CFU/mL	–	Chicken meat	[122]
	Au NPs	Colorimetric	–	10 pg/μL	–	–	[119]
Staphylococcus aureus	Ag NPs	DPV	10–10^6 CFU/mL	1 CFU/mL	–	Water	[123]
	SWCNTs	DPV	10–10^6 CFU/mL	13 CFU/mL	–	Milk	[124]
	GNDs	CV/DPV	–	0.1 nM	–	Fruit juice	[125]
	FNPs (UCNPs@GDN)	SFUCFS	10^3–10^8 CFU/mL	1.3 × 10^2 CFU/mL	70–118.2	Water/milk/beef	[126]
	Silica NPs	DPV	10–2 × 10^3 CFU/mL	11 CFU/mL	90–102	Milk	[127]
Listeria monocytogenes	Au nanostars	SERS- microfluidics	–	–	–	–	[128]
	Au NPs	SERS-LAMP-microfluidics	–	–	–	UHT milk	[129]
Aflatoxin	Fe3O4 NPs/Gr/CdTe QDs/CNTs	ECLIA	1–10^5 pg/mL	0.3 pg/mL	90–120	Milk	[50]
	ZnS QDs	MIP	2–20 μg/L	3.56 μg/kg	93	Fish feed	[51]
Ochratoxin	BFNS	Voltammetric	0.3–10 μg/mL	18 μg	98.8–103.3	Beer/grape juice	[130]
	ZnCdSe QDs	Turn off-on fluorescent sensor	0.5–80 ng/mL	0.33 ng/mL	98.3–103.7	Milk/coffee	[52]
	Au(core)@Au-Ag(shell) nanogapped/MNPs	SERS	0.01–50 ng/mL	0.004 ng/mL	92–112	Red wine	[131]
	CdTe QDs/MoS2 nanosheets	Fluorescence aptasensor	4–100 μg/mL	1 ng/mL	92–123	Red wine	[53]
	SWCNH	Fluorescence aptasensor	20–50 nM	17.2 nM	93–104.9	Red wine	[132]
pH changes	Halochromic NFs	ESP	–	–	–	–	[133]
	Halochromic NFs	ESP	–	–	–	Fish	[134]
	Halochromic NFs	ESP	–	–	–	Fish	[135]
Hydrogen	Pd decorated MnO_2nanowalls	Resistance change	–	10 ppm	–	–	[136]
Ammonia	SWCNTs	Chemiresistive detection	0–10 ppm	<0.5 ppm	–	Chicken/pork/cod	[137]
	Ag Nps	Plasmonic nanopaper	10–1000 μL	30.3 ppmv	–	Fish/meat	[138]
	SiO_2-reinforced PDA NFs	FS/colorimetric	–	7 ppm	–	Fish/meat	[139]
	rGO	Electrical resistance	–	1 ppm	–	–	[140]

ENFs = electrospun nanofibers; PAA = polyacrylic acid; PVA = polyvinyl alcohol; LAPS = light addressable potentiometric sensor; CFU = colony forming unit; d-Au NPs = dextrin-capped Au NPs; RFID = radio frequency identification; RPA = recombinase polymerase amplification; MNPs = magnetic NPs; UCNPs = upconversion NPs; MWCNTs = multi-walled carbon nanotubes; CV = cyclic voltammetry; rGO = reduced graphene oxide; DPV = difffrential pulse voltammetry; Ag NPs = silver NPs; SWCNT = single-walled CNTs; GNDs = graphene nano dots; FNPs = fluorescent NPs; UCNPs@GDN = guanidine-functionalized upconversion FNPs; SFUCFS = straightforward upconversion fluorescence sensing; Gr = graphene; CdTe QDs = cadmium tellurium quantum dots; ECLIA = electrochemiluminescent immunoassay; ECISP = electrochemical immunosensing platform; MIP = molecularly imprinted polymer; BFNS = black phosphorene nanosheets; SERS = surface-enhanced raman scattering; LAMP = loop-mediated isothermal amplification; SWCNH = single-walled carbon nanohorn; ESP = electrospinning; PDA = polydiacetylene; ppmv = part per million by volume; FS = forcespinning.

become one of the world's health problems due to its potential pathogenicity and resistance to antimicrobial drugs. Usually, 5% of all microbial food poisoning is caused by enterotoxins of this bacterium [141]. Aptamer-conjugated Ag NPs (Fig. 4c) [123], antibody-SWCNTs bioconjugate modified electrode [124], and paper based geno-interface incorporated with graphene nano dots (GNDs) and zeolites [125] are some sensors used successfully to detect this pathogen. Moreover, The use of FNPs made it possible to identify seven foodborne pathogens simultaneously, including *E. coli*, *Salmonella, Cronobacter sakazakii, Shigella flexneri, Vibrio parahaemolyticus, S. aureus,* and *L. monocytogenes*. Guanidine-functionalized upconversion (UCNPs@GDN) FNPs were applied to make this nanosensor for the quantifiable detection of these bacteria in actual samples of water, milk, and beef with appropriate recovery values (Fig. 4d) [126]. In another research, an electrochemical immunosensor based on nano mesoporous SiO_2 was applied to detect the bacterium. Based on differential pulse voltammetry (DPV) and electrochemical impedance spectroscopy (EIS), the LODs were 10 to 2 × 10^3 and 12 CFU/mL, respectively. This label-free sensor could determine the analyte within 20 min, and it was tested on the spiked milk sample [127].

4.1.3. Listeria monocytogenes

Listeria monocytogenes is one of the most serious foodborne pathogens due to its high mortality rate and ubiquity. According to reports, it has one of the highest mortality rates in Europe at 13.8% in 2017. The standard method for detecting this bacterium is a microbial culture, which takes 30–48 hours [142]. Therefore, it is valuable to have techniques that can show the presence of this bacterium in the sample in any situation. One of the attractive detection techniques that has been considered in recent years is the integration of surface enhanced Raman scattering (SERS) and microfluidic devices. This synergy is also known as lab-on-a-chip SERS (LoC-SERS) or nano/micro-optofluidics SERS. Hence, SERS measurements have been dramatically developed because processes previously performed on a large scale in the laboratory and prone to human error can now be conducted automatically and repeatably in nanoliter volumes. Besides, microfluidic platforms require detection methods that can be sensed in small volumes, and therefore, SERS is ideal for this responsibility [143]. In this regard, a study using Au nanostars and the combination of these two techniques succeeded in detecting *L. monocytogenes*. The Au nanostars synthesized were tagged with a Raman molecular probe. In the next step, the SERS-tagged Au nanostars were coated with a silica thin mesoporous layer and functionalized with a selective monoclonal antibody (mAb) for the detection of *L. monocytogenes*. A mixture of bacteria and tagged-NPs was incubated and injected into the microfluidic device placed under a Raman microscope. Then, the laser was concentrated in the center of the outlet channel. Notably, this strategy distinguishes

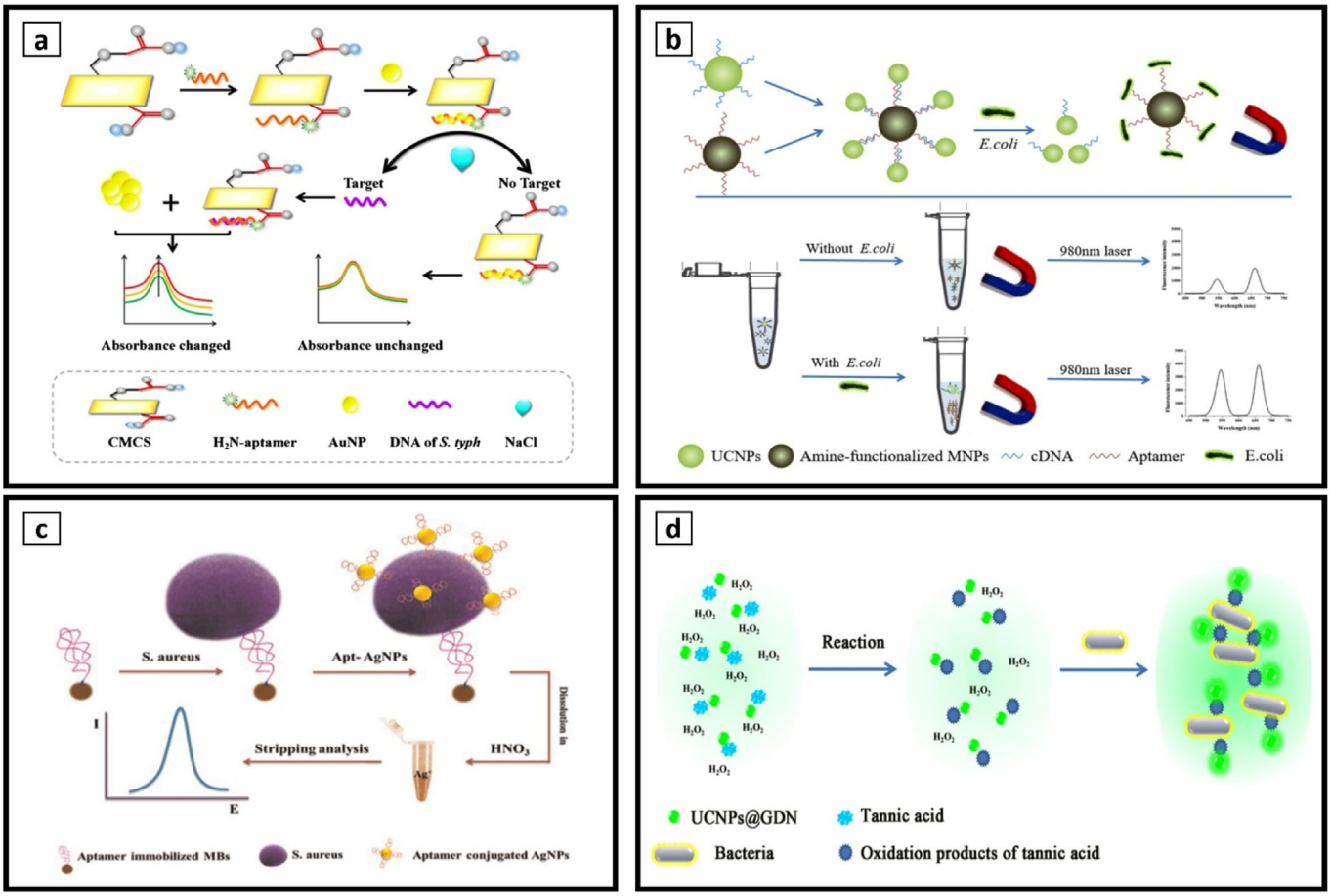

Fig. 4. (a) Schematic representation of carboxymethyl chitosan-aptamer-Au NPs composites for the colorimetric detection of *S. typh*. [121] (b) Schematic diagram of the aptamer based magnetic and upconversion NPs conjugated fluorescence sensor for screening *E. coli*. [117] (c) Schematic description of the aptamer-conjugated Ag NPs for electrochemical determination of *S. aureus*. [123] (d) Schematic illustration of bacteria sensor detection based on UCNPs@GDN FNPs [126].

L. monocytogenes from *L. innocua* in just 100 s [128]. In another investigation, a combination of loop-mediated isothermal amplification (LAMP) and SERS was applied to detect this pathogen in a buffer and ultra-high temperature milk, which is an outstanding option for DNA ultradetection. The researchers proposed an indirect SERS detection method employing multifunctional Au NPs based on the formation of pyrophosphate generated during the DNA amplification by LAMP. The use of LAMP facilitates the integration process in microfluidic devices since it does not require a temperature cycle [129].

4.2. Detection of toxins

Toxins are harmful substances produced by living organisms, including animals, plants, bacteria, and fungi. These materials are distinguished from industrial toxins in some respects and humans do not interfere in their production. Toxins do not convert to vapor and have very high toxicity relative to their weight. Fungal toxins (mycotoxins) are known to be highly biologically hazardous substances, such as aflatoxins and ochratoxins, which are important mycotoxins. Due to the high toxicity of these toxins, their rapid and timely detection in human food and animal feed is a major necessity. Many of the methods used to detect aflatoxins and ochratoxins are advanced instrumental methods or highly specialized biological methods that, in addition to time and high cost, require experienced personnel to perform the tests, while in many cases where it is necessary to identify the toxins, these devices are not available and make the detection process more difficult [144].

4.2.1. Aflatoxins

Aflatoxins are among the most serious fungal toxins that cause destructive effects on the biological systems, they are mainly produced by different species of the fungus *Aspergillus* belonging to the Flavi group. Four different aflatoxins are commonly produced in plant products such as pistachios, peanuts, and corn, which are called aflatoxins B1, B2, G1, and G2. However, other biologically altered aflatoxins, such as aflatoxins M1 and M2, may also be present in milk [145]. In 2013, Gan et al. designed an extremely sensitive immunosensor to detect aflatoxin M1. At first, IO NPs stabilized on graphene oxide were used as adsorbents for aflatoxin M1. Then, using an aflatoxin M1 antibody and cadmium tellurium quantum dots (CdTe QDs) as a detector, they were able to detect aflatoxin M1 with a LOD of 0.3 pg/L [50]. Recently, room temperature phosphorescent has been applied to detect and measure aflatoxins in fish feed using molecularly imprinted polymer (MIP) – Mn-doped ZnS quantum dots with a LOD of 3.56 μg/kg. This simple, low-cost technique has been suggested for assessing the aflatoxins in complex materials [51].

4.2.2. Ochratoxin

One of the most important mycotoxins is ochratoxin, produced by some fungi of the genus *Penicillium* and *Aspergillus* in food and feed, especially in areas with cold and humid climates. Its main forms are ochratoxin A, B, and C. The most important and common form of this group is ochratoxin A (OTA), and its presence has been reported in a wide range of foods, including cereals, coffee, dried fruits, grape juice,

legumes, milk, and processed and dried meat products [146]. Given the potential health risks of ochratoxin, many countries and the European Union (EU) have set a low threshold for the possible presence of ochratoxin in food. The maximum allowable level of this toxin is 10, 2, 3, and 0.5 ng/g in dried fruits and coffee, grape juice and grape products, cereals and their products, and infants food, respectively.

A nanosensor based on black phosphorene nanosheets (BPNS) was designed to detect the OTA in food samples such as beer and grape juice, which was based on the voltammetric analysis. This modified electrochemical electrode showed a great linear reaction to OTA in the range of 0.3–10 μg/mL with a LOD of 18 μg under optimal conditions. The described mechanism for the electrocatalytic oxidation of OTA is an irreversible electrochemical response with an adsorption-controlled process, and the nitrogen amide atom in OTA is oxidized to N+O- [130]. Quantum dots and self-assembled porphyrin were also employed to fabricate a nanosensor to detect OTA. It was able to identify the toxin in milk and coffee within 5 min during a two-step process [52]. Other detection methods such as SERS aptasensor [131], and fluorescent aptasensor [53,132] are also applied to detect OTA, as shown in Fig. 5a.

4.3. Detection of pH changes to reveal spoilage

One of the modern technologies that has the potential to revolutionize the packaging industry is the use of sensors and detectors whose color changes as a result of variations in the characteristics of the packaged product. One of these detectors is halochromic material whose its color changes in response to pH variations. In fact, the word chromic is defined as a substance that can change its color reversibly under the influence of a factor. For halochromic sensors, the cause of the color change is the pH value. In this type of smart packaging, as soon as the spoilage begins, accompanied by pH changes, the color of the packaging changes and warns the consumer. This system is much more accurate and reliable than the expiration date.

One of the applications of ENFs is in halochromic packaging. For example, in a study by Devarayan and Kim (2015), an eco-friendly, reversible, and universal sensor based on electrospun cellulose nanofibers with natural pigments extracted from red cabbage (anthocyanin) was investigated. The results showed this sensor could detect pH values in the range of 1–14 and its sensitivity to pH was stable at different temperatures and for a long time [133]. Moreover, cellulose acetate nanofibers have been used to detect the spoilage of *Rainbow Trout* [134], as depicted in Fig. 5b. In another study, a nanosensor based on zein ENFs was used to detect the fish spoilage. No color changes occurred in the first four days of storage, but later, a light purple color was observed in the sensor by the naked eye [135].

4.4. Detection of gases to reveal spoilage

There have been many studies in the field of gas sensors in which, a wide range of target gases have been identified. Many of these gases, such as the NO_x family and CO, are potentially dangerous and cause death [147]. Detection of some other types of gases such as oxygen [148] and hydrogen [136] have also been used in the process control and industrial production. Ammonia gas, formed from the decomposition of organic matter, is one of the signs of food spoilage, released in minimal amounts (<30 ppm) as a result of food spoilage. High-efficient sensors and appropriate responses are required to detect such small amounts of ammonia gas.

There are many methods for detecting gases with the help of sensors, including electrochemical sensors, mass sensors, and optical sensors. Although non-functionalized SWCNTs are known to detect amines chemiresistively, a study improved the sensitivity and specificity of nanotubes to amines by functionalizing them. Chemiresistive detectors made of cobalt porphyrin/SWCNTs composites were used to detect biogenic amines (BA) such as putrescine and cadaverine and investigate the spoilage of raw meat. The reasons for the rapid detection of low concentrations of amines with high sensitivity include changes in the oxidation state of the metal, the electron-withdrawing character of the porphyrin ligand, and the counteranion [137]. In another study, a plasmonic membrane was used as a hybrid material based on Ag NPs embedded in bacterial cellulose. When the nanopaper was exposed to ammonia gas released due to meat and fish spoilage, the population density of Ag NPs was reduced which was associated with a decrease in UV-Vis spectroscopy absorption. In these conditions, the color of plasmonic nanopaper was turned from amber to grey. LOD also changed from 30.3 to 0.574 ppmv of ammonia at higher exposure time (2–8 h) [138]. Furthermore, researchers have constructed polydiacetylene (PDA) nanofibers using the forcespinning (FS) method for the optical sensing of BA. In this way, the freshness of meat products can be monitored by changing the color from blue to red with a LOD of about 7 ppm in 7 min. This fluorescent sensor is more sensitive than other methods of detecting this analyte such as chromatographic and chemiluminescence, which is able to detect 100 ppm in the most sensitive cases [139]. One of the recent studies for ammonia detection is a sensor based on nanocomposites of phosphate-functionalized rGO/polyaniline immobilized on microstrip resonators with a low LOD of 1 ppm [140].

5. Nanosensors for detection of food adulteration

5.1. Detection of food additives

One of the critical aspects of food health monitoring is the control of the amount and type of food additives added by producers into various foods. Food additives vary widely, and some of them could have severe detrimental effects on human health. For this reason, the use of some additives is prohibited, so-called illegal food additives [149]. Conventional methods for the detection and measuring of different food additives include thin-layer chromatography [150], DPV [151], adsorptive voltammetry [152], capillary electrophoresis [153], traditional chromatography [154], and high-performance liquid chromatography [155]. The long sample preparation process and inefficiency in multi-color mixtures are among the weaknesses of most of these methods. Given that the allowable values for most additives are in the range of a few ppm or less, regulatory organizations must have appropriate and accurate detection methods for identifying and determining the amounts of food additives [156]. Therefore, nanomaterial-based sensors could be a promising solution.

5.1.1. Detection of dyes

One of the most widely used types of food additives is food colorants, to compensate for the natural color of the food, destroyed during the production process as well as during the storage period of the product until consumption. Food colorants in the food industry are divided into two categories [157]: (1) natural dyes that have a natural origin and formulation; and (2) synthetic dyes which are actually chemical compounds produced in the chemical and dye industries. The molecular structure of these dyes generally differs significantly from that of natural dyes. Synthetic dyes have advantages over natural dyes (for example, lower price and higher stability to light, oxidation, and pH changes) and may be preferred [158]. Therefore, the possibility of excessive amounts of these additives in food products increases. Due to the biological effects of these dyes and the dangers of overconsumption, it is critical to precisely control their amounts in food products [159].

Sudan I (1-phenylazo-2-naphthol) is a synthetic azo-colorant dye, frequently found in adulterated chili powder, curry products, and sauces. Yin et al. (2011a) developed a simple and sensitive electrochemical method for measuring Sudan I dye based on the carbon electrode modified with cyclic voltammetric (CV) magnetite NPs. The modified sensor compared to the unmodified carbon electrode clearly showed the electrocatalytic activity towards Sudan I oxidation, corresponding to an increase in the peak oxidation current and a decrease in the peak oxidation potential [160]. According to other studies, it has also

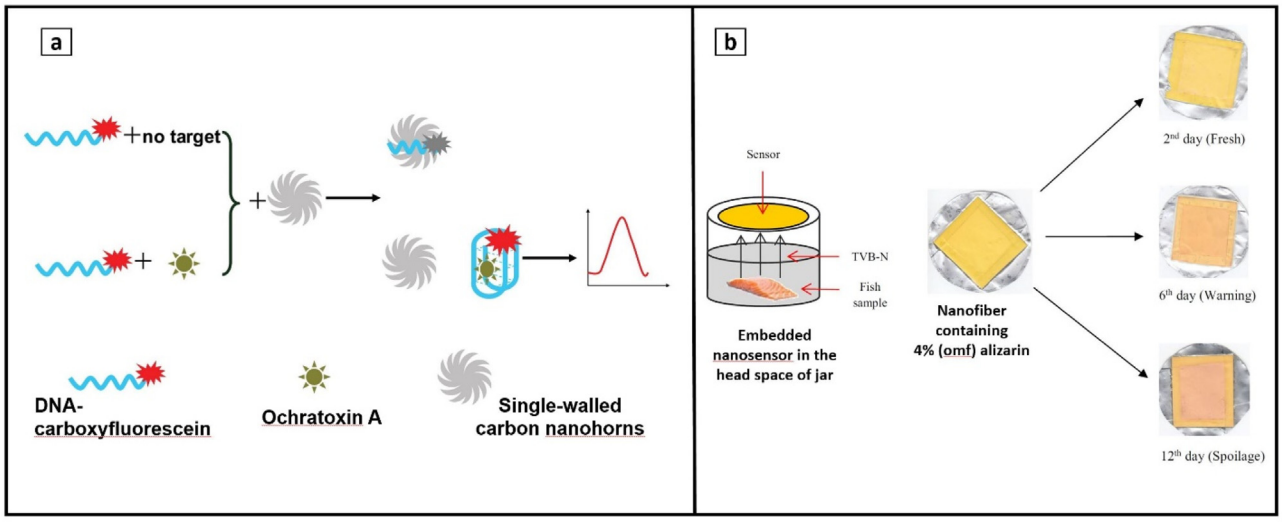

Fig. 5. Schematic representation of (a) the single-walled carbon nanohorns -based fluorescent ochratoxin A detection [132], and (b) a halochromic sensor of cellulose acetate nanofibres and alizarin for detection of fish spoilage [134].

been suggested to use the glassy carbon electrode modified with graphene (CV) [161], rGO/Au NPs (DPV) [162], and electrochemically rGO (linear sweep voltammetry) [163] to detect Sudan I. This adulterant is also detectable by platinum NPs decorated graphene-β-cyclodextrin modified electrode with a LOD of 1.6 nM and sensitivity of 2.82 μA μM^{-1} cm^{-2} [164]. Recent advances have investigated the use of La3+-doped Co_3O_4 nanocubes [165] and ZnO-CuO nanoplates [166] to modify screen-printed electrode sensing. Besides, the researchers were able to prepare bismuth tungstate (Bi_2WO_6) nanosheets modified glassy carbon electrode with a high sensitivity and low LOD of 3.056 mu A mu M^{-1} and 0.002 mu M, respectively [167].

Sunset yellow and tartrazine are also toxic synthetic dyes that can be detected by nanosensors. Yang and Li [168] prepared hexadecyl trimethyl ammonium bromide functionalized GO/multiwalled CNTs modified glassy carbon electrode (CTAB-GO/MWNT/GCE) that can simultaneously detect sunset yellow and tartrazine with a LOD of 1×10^{-8} M and 5×10^{-9} M, respectively. Also, the operational parameters optimized in this study included accumulation time, solution pH, and scan rate, which affect the analytical performance of determination. In another study, green synthesized fluorescent carbon dots were employed for the selective detection of tartrazine in food samples, which were spherical carbon dots with an average diameter of 5 nm [54]. Moreover, an electrochemical sensor based on β-cyclodextrin/ionic liquid/Au NPs functionalized magnetic GO was used to detect sunset yellow with a wide linear range from 5.0×10^{-9} to 2.0×10^{-6} mol/L and a LOD of 2.0×10^{-9} mol/L [169]. The most recent studies that can be mentioned are novel and high-sensitive graphene/poly(L-phenylalanine) [170] and spark generated molybdenum NPs [171] modified graphite electrodes with recovery values of 98–104% and 94–109%, respectively. An overview of the application of nanosensors for the detection of food adulteration is provided in Table 3.

5.1.2. Detection of preservatives

Preservatives are natural or synthetic chemicals added to food to preserve and reduce spoilage (loss of quality or nutritional value) and food degradation by microorganisms [191]. Parahydroxybenzoates, or parahydroxybenzoic acid esters, commonly known as parabens, have been used as a preservative in various industries for more than seventy years. Parabens have preservative effects and are easily added to a variety of pharmaceutical and food products since they do not cause any odor or taste and do not change the color or firmness of the product. The integration of N-methacryloyl-Lphenylalanine into the polymeric structure makes it possible to mimic the biological recognition ability of biological molecules through secondary interactions via the aromatic ring in its structure and carboxylic acid groups. Accordingly, an electrochemical sensor was prepared using a polymer nanofilm modified screen-printed Au electrode to detect parabens. Under optimal conditions, the linear working range was found to be 1–30 μM with a LOD as low as 0.706 μM [172]. Sulfite is an inorganic anion, used in the food and pharmaceutical industries as a preservative and antioxidant, and in the tea industry as an antibacterial agent. Due to its potential toxicity and harmful effects on human health and other organisms, the amount of sulfite in food and beverages should be controlled. In a study, cetyltrimethylammonium bromide fluorescent organic NPs (CTAB-FONs) were applied as a nanosensor to detect this substance in the aqueous medium, food samples, and cells with an ultrafast detection time (15 s) and an ultralow LOD (7.4 nM). The paper-based device of this nanosensor is also provided. This diagnosis was provided by the Michael addition reaction of sulfite to CTAB-FONs [173].

5.2. Detection of sugars

One of the biggest frauds in the juice industry is the addition of cane and beet invert sugars to fruit juices to imitate the natural sucrose-glucose-fructose profile. Numerous investigations have been reported for the detection of sucrose by electrodes with the three types of enzymes, including invertase, glucose oxidase, and peroxidase/mutarotase. However, they have limitations such as cross-reactivity with feedback enzyme inhibition and a low sensitivity [174]. Li et al. [176] evaluated the glucose detection mechanism using systems based on semiconductor SWCNTs with a paradigmatic sensor configuration computationally and reported that the sensitivity of these systems to this analyte is higher than the sensitivity of metallic nanotube-based systems. In another interesting research, an electrochemical platform was fabricated for saccharide or sucrose analysis using biocomposite of nanomaterials. For this purpose, hydrogels were prepared from two natural polysaccharides, gum Arabic and cornflour, and reinforced by platinum NPs anchored with carboxyl-functionalized CNTs. Then, invertase and glucose oxidase were entrapped in the gum Arabic-corn flour hybrid matrix. Screen-printed carbon electrodes were modified with the aim of developing a highly sensitive electrochemical biosensor system for detecting sucrose using this enzyme-nanocomposite matrix. The reported LOD was 1×10^{-9} mol/L [175].

Table 3
Examples of nanomaterial-based sensors for the detection of adulteration in food analysis.

Target analyte	Nanomaterial	Method/technique	Linear range	Limit of detection	Recovery (%)	Food matrix	Reference
Sudan I	Fe_3O_4 NPs/GCE	DPV	0.01–20 μM	0.001 μM	96.2–103.6	Chilli powder/sauce/duck egg yolk	[160]
	rGO/GCE	LSV	0.04–8.0 μM/L	0.01 μM/L	84–110	Chili sauce/tomato sauce	[163]
	Gr/β-CD/PtNPs/GCE	DPV	0.005–66.68 μM	1.6 nM	96–99.3	Chili powder/chili sauce/tomato sauce/ketchup	[164]
	La^{3+}-doped Co3O4 NCs/SPE	CV	0.3 to 300.0 μM	0.05 μM	95.6 to 104	Tomato paste/ketchup sauce/chilli powder	[165]
	ZnO-CuO NPls/SPE	DPV/CV	0.6 to 600 μM	0.18 μM	97.1–103.2	Tomato paste/ketchup sauce/chilli powder	[166]
	Bi_2WO_6 Nanosheets/GCE	DPV	0.02 to 114.6 μM	0.002 μM	96.8–98.6	Apple juice/chili powder	[167]
Catechol	GO@PDA–AuNPs	CV	0.3–67.55 μM	0.015 μM	96–97.5	Water	[161]
Dopamine	Gr/β-CD/GCE	DPV	0.1–58.5 μM	0.011 μM	about 97.6% in human serum sample and 96.1% in pharmaceutical samples	Biological samples	[162]
Sunset yellow	GO/MWCNTs/GCE	DPV	10^{-7}–2×10^{-5} M	10^{-8} M	90 to 110	Soft drink	[168]
	Au NPs	CV/EIS	5×10^{-9}–2×10^{-6} mol/L	2×10^{-9} mol/L	97–105	Water sample/mirinda drink/minute maid	[169]
	Mo NPs	DPV(Ox)	0.005–0.25 nM	2 nM	96.3 to 109	Orange sweetie/Green sweetie/cocktail margarita	[130]
Tartrazine	GO/MWCNTs/GCE	DPV	3×10^{-8}–6×10^{-7} M	5×10^{-9} M	93–111	Soft drinks	[168]
	CQDs	Fluorescence analysis	0.25 to 32.5 μM	73 nM	87.3–106.6	Steamed buns/honey/candy	[54]
	Gr/PLPA/PGE	DPV	1.54 to 5.14 μM	1.54 μmol/L	98.71–104.44	Orange juice	[170]
	Mo NPs	DPV(Ox)	0.005–0.25 nM	2 nM	94.5–106	Orange sweetie/green sweetie/cocktail margarita	[171]
Paraben	PHEMA-MAPA nanofilm	CV/SWV	1–30 μM	0.706 μM	91.88–119.60	–	[172]
Sulfite	CTAB-FO NPs	Fluorescence analysis	2–7 μM	7.4 nM	96.6–102.4	Granulated sugar	[173]
Sucrose	Au NPs	Voltammetric	–	9 μM	–	–	[174]
	Carboxylated-MWCNT	SPCE	1×10^{-4}–1×10^{-9} mol/L	1×10^{-9} mol/L	–	Commercial fruit, vegetable, and mix juice	[175]
Glucose	CNTs	Electrical conductance	–	300 nM	–	–	[176]
Melamine	Au NPs	Colorimetric	0.1–2 mg/L	0.05 mg/L	95–105	Milk	[177]
	Crown ether-Au NPs	Colorimetric	10–500 ppb	6 ppb	98.4–105.6	Milk	[178]
	Au NPs	Colorimetric	–	1 ppb	–	Milk	[179]
	Au NPs	Chemiluminescence resonance energy transfer	3.2×10^{-12}–3.2×10^{-7} mol/L	3×10^{-13} mol/L	94.1 to 104.2	Milk	[180]
	Ag NPs	Colorimetric	4–170 μM	2.32 μM	88.83–114.29	Milk	[181]
	Ag NPs	Colorimetric	0.033–1.50 mg/L	0.009 mg/L	61.9–96.3	Milk	[182]
	Ag NPs	Colorimetric	0.2–1.6 mg/L	0.04 mg/L	92.5–99.4	Milk	[183]
	Ag NPs	Colorimetric	0–5 ppm	0.1 ppm	–	Milk	[184]
	Ag NPs	Colorimetric probe	500–10000 ppb	252 ppb	96–122	Milk	[185]
	Ag NPs	Colorimetric/interference-biosynthesis	0.1–5 ppm	0.5 ppm	96	Milk	[186]
Urea	NF/Ag-N-SWCNTs/GCE	Non-enzymatic electrochemical detection	66 nM–20.6 mM	4.7 nM	95.3	Milk/water	[187]
	GNPlt-CNT	Amperometry	0.1–0.8 mg/mL	33 μA $(mg/mL)^{-1}$	–	–	[188]
	GNPlts/GND	SPCE	0.1–0.9 mg/mL	0.005 mg/mL	–	Water	[189]
	PA6-PPy NFs/ZnO	ESP	0.1–250 mg/dL	0.011 mg/dL	97–99	Milk	[190]

NPs = nanoparticles; GCE = glassy carbon electrode; DPV = differential pulse voltammetry; GO = graphene oxide; PDA = polydopamine; AuNPs = gold NPs; CV = cyclic voltammetry; CD = cyclodextrin; rGO = reduced GO; LSV = linear sweep voltammetry; Gr = graphene; PtNPs = platinum nanoparticles; NCs = nanocubes; SPE = solid-phase extraction; NPls = nanoplates; Bi_2WO_6 = bismuth tungstate; MWCNTs = multi-walled carbon nanotube; CQDs = carbon quantum dots; EIS = electrochemical impedance spectroscopy; PLPA = poly(L-phenylalanine); PGE = pencil graphite electrode; Ox = oxidative determination; Mo NPs = Molybdenum NPs; PHEMA-MAPA = poly-(2-hydroxyethyl methacrylate-N-methacryloyl-L-phenylalanine); SWV = square wave voltammetry; CTAB = cetyltrimethylammonium bromide; FO NPs = fluorescent organic NPs; NF = Nafion; N = nitrogen doped; GNPlt = graphene nanoplatelets; GND = graphitized nanodiamond; SPCE = screen-printed carbon electrode; PA6 = polyamide 6; PPy = polypyrrole; ZnO NPs = zinc oxide nanoparticles; ESP = electrospinning.

5.3. Detection of melamine

Melamine (1,3,5-triazine-2,4,6-triamine, $C_3H_6N_6$) is an organic chemical-based substance commonly found in white crystals form which contains 66.6% nitrogen. This substance is illegally added into food products, particularly milk and dairy products, to provide a high incorrectly reading in measuring total protein, since standard tests such as Kjeldahl and Dumas measure the amount of food protein through measuring the nitrogen. Thus, these tests are unable to detect nitrogen from non-protein sources and nitrogen-rich compounds such as melamine to foods [76]. In the year 2007, melamine was discovered in wheat gluten and protein fortified rice exported from China. It was used in animal feed in the United States and killed many dogs and cats for kidney failure [192]. Besides, in the year 2008, thousands of Chinese infants and children were poisoned and at least six of them confirmed to have died from consuming melamine-contaminated infant milk powder. Other cases of melamine adulteration in eggs and different types of milk-based products such as biscuits, candies, and yogurt desserts have also been reported [193]. The maximum limit of melamine content in infant formula is 1.0 ppm, whereas, for other foods and animal feeds, it is 2.5 ppm [179].

Gas chromatography/mass spectrometry (GC/MS) is the official method for melamine detection specified by the FDA, which has quantification limits of 0.05–10 ppm. Other methods, such as liquid chromatography, infrared spectroscopy, and electrochemical methods, have been employed for the detection of melamine [182]. Although each of these methods has high sensitivities, most of them are time-consuming and expensive. In colorimetric evaluation, Au NPs have been used more for their unique inherent properties, including simple preparation, high biocompatibility, stability, and extinction coefficient. According to this fact, extensive studies have been conducted on the detection of this adulterant using Au NPs in simple, low-cost, and highly sensitive methods with a LOD of 0.05 ppm [177], 6 ppb [178], and even 1 ppb [179]. As shown in Fig. 6a, the main mechanism governing most of these methods is that the colloidal solution of Au NPs has a red color, indicating proper dispersion of Au NPs. After exposure to melamine, these NPs aggregate, and as a result the color of the solution changes to the blue [177].

Au NPs-based chemical resonance energy transfer was also proposed as a novel strategy for the highly sensitive detection of melamine. Based on this technique, the chemical signal of bis(2,4,6--trichlorophenyl) oxalate (TCPO)–hydrogen peroxide–fluorescein is attenuated in the presence of Au NPs, and when NPs are exposed to melamine, the chemical signal increases. As a result, chemiluminescence severity is restored. With this method, the values of 3.2×10^{-12} to 3.2×10^{-7} melamine can be measured with a LOD of 3×10^{-13} mol/L [180].

Ag NPs similar to Au NPs aggregate in the presence of melamine and result in a yellow-to-red color change, due to the shift of surface plasmon band to longer wavelengths. Some studies have been done on the detection of melamine using Ag NPs. Label-free Ag NPs were used as a probe with a LOD of 2.32 μM. In this study, the borohydride reduction method was used to synthesize Ag NPs, which leads to homodisperse of Ag NPs. The negatively charged citrate ions cover Ag NPs and the electrostatic force counteracts the *Van der Waals'* force effects between the molecules [181]. An interesting strategy was suggested for the synthesis of stable colloidal Ag NPs *via* the use of factorial design to optimize the concentrations of $AgNO_3$ and $NaBH_4$. The stability of synthesized NPs with a mean diameter of 14 nm was reported for at least 5 days at 4 °C. Strong interactions were established between the Ag NPs and the amine groups, which increased the sensitivity of detection for melamine in milk products because no stabilizing agents were used in this method. NPs synthesized by this method have been applied in the detection of melamine with a LOD of 0.009 mg/L [182].

In other studies, rapid sensing of melamine in milk by 35 nm diameter unmodified Ag NPs [183] and green synthesized Ag NPs [184] were reported with a LOD of 0.04 mg/L and 0.1 ppm, respectively. $AgNO_3$ was used as a precursor and ascorbic acid as a reducing agent for green synthesis of Ag NPs in the mentioned research. Dispersed Ag NPs give strong absorption in UV–Vis spectra around 397 nm. On the other hand, the exocyclic amino groups of melamine (positive charge) attach to these citrate ions on the surface of Ag NPs (negative charge). Thereby, hydrogen bonding between Ag NPs and melamine molecules causes aggregation of Ag NPs which produce visual color changes with the appearance of new absorption maxima around 540 nm as shown in Fig. 6b. More and more Ag NPs aggregate as the concentration of melamine increases and the absorption spectra around 540 nm increases simultaneously [183]. The green synthesis of Ag NPs with leaf extracts, including *Jatropha gossypifolia* [185] and *Parthenium* [186] also yielded good results for the single-stage melamine detection. In general, melamine detection with Ag NPs is performed in two steps. The first step requires the synthesis and functionalization of Ag NPs, and the second step involves the detection of melamine using functionalized Ag NPs. Green synthesis of Ag NPs is not only an eco-friendly process but also a rapid (<20 s) and one-step method for analyte detection. In this

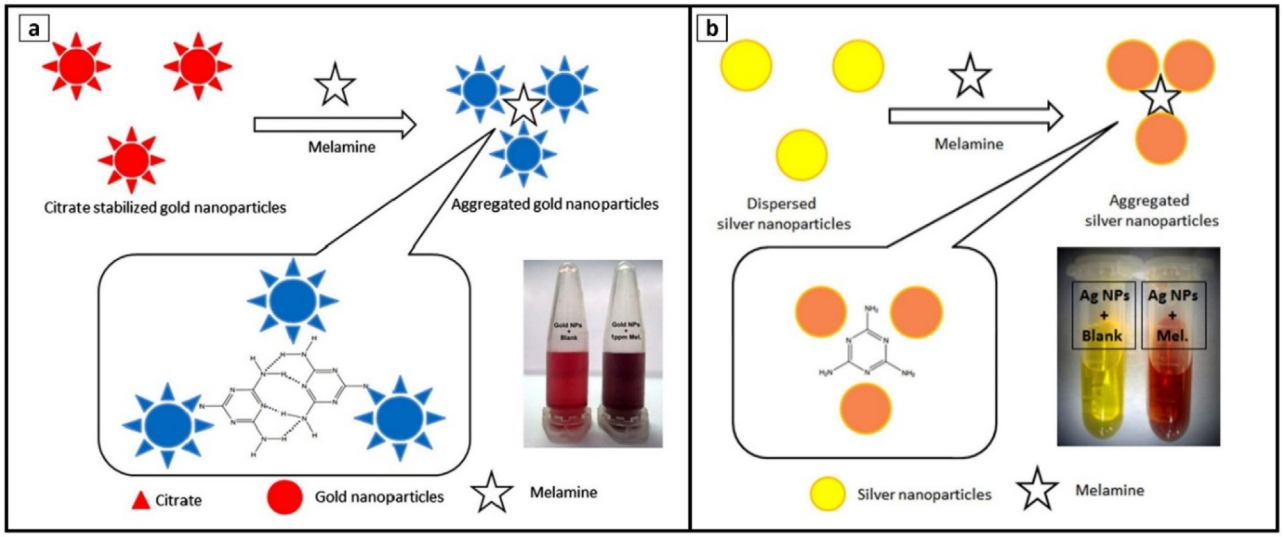

Fig. 6. Schematic representation for the mechanism of melamine detection in milk products using (a) gold nanoparticles [177]; and (b) silver nanoparticles [183].

strategy, the analyte interferes with the biosynthesis of the NPs and then is detected by the NPs.

5.4. Detection of urea

Urea is another adulterant that is added to diluted milk to show a higher nitrogen content. Naturally, the concentration of urea in milk is 3.1 to 6.6 mM, whereas the maximum amount of urea that can be in milk is between 0.2 and 0.4 mg/mL. More than this value, it is considered an adulteration. Enzyme-based sensors are commonly applied to detect this analyte [194–198]. As the research progressed, these enzymatic biosensors were improved over the years 2008 to 2017, so that their sensitivity was changed from 124.84 μA mM^{-1} cm^{-2} to 0.32 nA mM^{-1}, their LOD from 499 to 2 μM, and the response time from 10 to 3 s. These enzymatic techniques have several drawbacks, including high construction costs and inadequate stability.

A non-enzymatic electrochemical method to detect urea has been reported in which a glassy carbon electrode was modified using Ag NPs decorated nitrogen-doped SWCNTs (Ag-N-SWCNTs) and a layer of Nafion. Higher sensitivity, a lower LOD, and fast response time of this fabricated electrode were reported as 141.44 $\mu AmM^{-1}cm^{-2}$, 4.7 nM, and 3 s, respectively. This modified electrode is also capable of storage under ambient conditions without loss of activity and exhibited high selectivity toward urea with excellent repeatability and reproducibility (Fig. 7a) [187]. In another study to detect urea, graphene nanoplatelets conjugated with urease were applied. Urea is hydrolyzed by urease, producing ammonium and carbonic ions. The principal aim of this investigation was to detect these ions effectively. The conjugated compound was immobilized on a CNTs- covered electrode, which can be applied around 20 times [188].

Urease-immobilized graphene nanoplatelets and graphitized nanodiamonds nanocomposites have also utilized for electrochemical detection of this analyte with 20 s response time and a LOD of 5 μg/mL. The proposed sensor can directly detect urea and has advantages such as higher enzyme loading, higher charge transfer to the electrode surface, and more efficient surface area, which leads to higher sensitivity

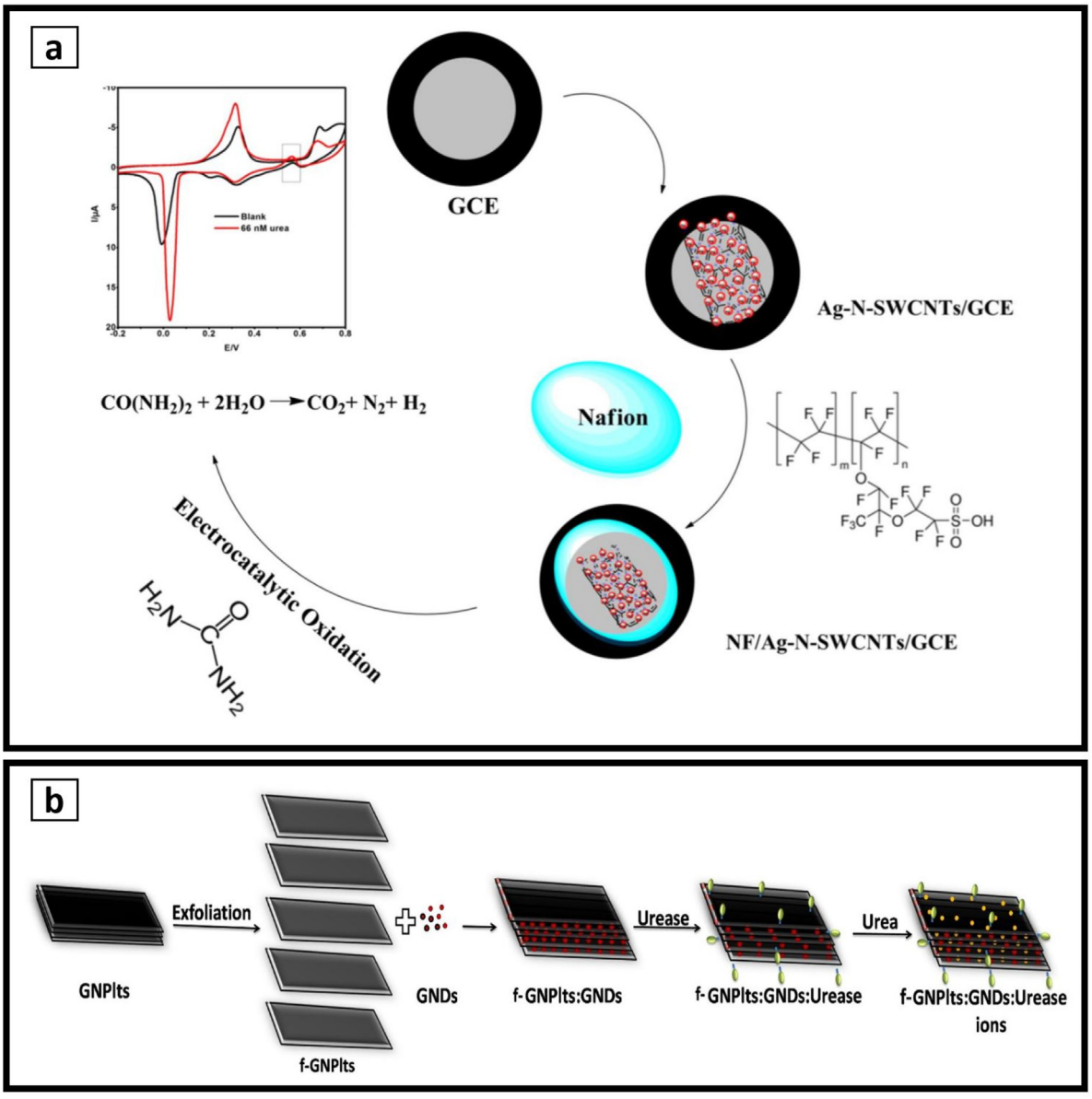

Fig. 7. (a) Schematic illustration of non-enzymatic electrochemical detection of urea on Ag Nps anchored N-doped SWCNT modified electrode [187]. (b) Schematic representation of graphene nanoplatelet/graphitized nanodiamond-based nanocomposite for electrochemical sensing of urea [189].

(Fig. 7b) [189]. Another way to detect urea is to use ENFs modified with ZnO NPs and enzyme urease applying a simple electrostatic process. ZnO results in hydrogen bonding or electrostatic interactions between the carboxylic groups (-COOH) from the Liosperse 511 (dispersing agent) and the amino groups from PPy and amide nitrogen from PA6, respectively. A biosensor is designed to detect urea using this strategy that has a LOD of 0.011 mg/dL, which is lower than other similar studies (2–13.5 mg/dL) [190].

6. Conclusions and future outlook

Nanomaterials have unique sensory properties, the most important of which as described in this paper, include the optical and magnetic properties of NPs, the thermal and electrical properties of CNTs, the electron transfer of NWs, and the high porosity of ENFs. An overview of their application in the design of sensors for the detection of spoilage and adulteration in food products and their recent developments were presented. The fabricated nanosensors can quickly, accurately, and selectively detect analytes with a minimum sample. Among the various nanomaterials, metal NPs, mainly Au and Ag, and CNTs have been used widely in this field. Of course, new nanostructures such as graphene and its derivatives will undoubtedly lead to future advances due to their unique surface features. Moreover, the use of pH-sensitive nanofiber sensors in the field of smart food packaging and its application in spoilage monitoring is novel. The ability to detect complex matrices, reduce costs, and portable features are among the goals that can be developed in the future for the design and fabrication of nanosensors. Also, economic points should be considered for the commercialization and scale-up of these sensors for the food industry and regulatory organizations responsible for the monitoring of food quality and safety.

Declaration of Competing Interest

None.

References

[1] Bahrami A, Moaddabdoost Baboli Z, Schimmel K, Jafari SM, Williams L. Efficiency of novel processing technologies for the control of Listeria monocytogenes in food products. Trends Food Sci Technol 2020;96:61–78.
[2] Lewis E, Hudson J, Cook N, Barnes J, Haynes E. Next-generation sequencing as a screening tool for foodborne pathogens in fresh produce. J Microbiol Methods 2020:105840.
[3] López-Campos G, Martínez-Suárez JV, Aguado-Urda M, López-Alonso V. Detection, identification, and analysis of foodborne pathogens. Microarray detection and characterization of bacterial foodborne pathogens. Springer; 2012. p. 13–32.
[4] Sharma D, Nagpal A, Pakade YB, Katnoria JK. Analytical methods for estimation of organophosphorus pesticide residues in fruits and vegetables: a review. Talanta 2010;82:1077–89.
[5] Ahumada O, Villalobos JR. Application of planning models in the agri-food supply chain: a review. Eur J Operat Res 2009;196:1–20.
[6] Spink J, Ortega DL, Chen C, Wu F. Food fraud prevention shifts the food risk focus to vulnerability. Trends Food Sci Technol 2017;62:215–20.
[7] Alagarasi A. Chapter-introduction to nanomaterials. Indian Institute of Technology Madras; 2013; 1–24.
[8] Pan M, Yin Z, Liu K, Du X, Liu H, Wang S. Carbon-based nanomaterials in sensors for food safety. Nanomaterials 2019;9:1330.
[9] Qu J-H, Wei Q, Sun D-W. Carbon dots: Principles and their applications in food quality and safety detection. Crit Rev Food Sci Nutr 2018;58:2466–75.
[10] Shi X, Wei W, Fu Z, Gao W, Zhang C, Zhao Q, et al. Review on carbon dots in food safety applications. Talanta 2019;194:809–21.
[11] Krishna VD, Wu K, Su D, Cheeran MC, Wang J-P, Perez A. Nanotechnology: review of concepts and potential application of sensing platforms in food safety. Food Microbiol 2018;75:47–54.
[12] Chen Q, Zhu L, Chen J, Jiang T, Ye H, Ji H, et al. Recent progress in nanomaterial-based assay for the detection of phytotoxins in foods. Food Chem 2019;277:162–78.
[13] Inbaraj BS, Chen B. Nanomaterial-based sensors for detection of foodborne bacterial pathogens and toxins as well as pork adulteration in meat products. J Food Drug Analysis 2016;24:15–28.
[14] Bülbül G, Hayat A, Andreescu S. Portable nanoparticle-based sensors for food safety assessment. Sensors 2015;15:30736–58.
[15] Ghasemi-Varnamkhasti M, Apetrei C, Lozano J, Anyogu A. Potential use of electronic noses, electronic tongues and biosensors as multisensor systems for spoilage examination in foods. Trends Food Sci Technol 2018;80:71–92.
[16] Mercante LA, Scagion VP, Migliorini FL, Mattoso LH, Correa DS. Electrospinning-based (bio) sensors for food and agricultural applications: a review. TrAC Trends Anal Chem 2017;91:91–103.
[17] Mustafa F, Andreescu S. Nanotechnology-based approaches for food sensing and packaging applications. RSC Adv 2020;10:19309–36.
[18] Ghatak S. Strategies for elimination of foodborne pathogens, their influensive detection techniques and drawbacks. Meat quality analysis. Elsevier; 2020. p. 267–86.
[19] Joyner JJ, Kumar DV. Nanosensors and their applications in food analysis: a review. Int J SciTechnol 2015;3:80.
[20] Kuswandi B, Futra D, Heng L. Nanosensors for the detection of food contaminants. Nanotechnology applications in food. Elsevier; 2017. p. 307–33.
[21] Omanović-Mikličanina E, Maksimović M. Nanosensors applications in agriculture and food industry. Bull Chem Technol Bosnia Herzegovina 2016;47:59–70.
[22] Shafiq M, Anjum S, Hano C, Anjum I, Abbasi BH. An overview of the applications of nanomaterials and nanodevices in the food industry. Foods 2020;9:148.
[23] Srivastava AK, Dev A, Karmakar S. Nanosensors and nanobiosensors in food and agriculture. Environ Chem Lett 2018;16:161–82.
[24] Yin PT, Kim T-H, Choi J-W, Lee K-B. Prospects for graphene–nanoparticle-based hybrid sensors. Phys Chem Chem Phys 2013;15:12785–99.
[25] Adhikari B-R, Govindhan M, Chen A. Carbon nanomaterials based electrochemical sensors/biosensors for the sensitive detection of pharmaceutical and biological compounds. Sensors 2015;15:22490–508.
[26] Rotariu L, Lagarde F, Jaffrezic-Renault N, Bala C. Electrochemical biosensors for fast detection of food contaminants–trends and perspective. TrAC Trends Anal Chem 2016;79:80–7.
[27] Koedrith P, Thasiphu T, Tuitemwong K, Boonprasert R, Tuitemwong P. Recent advances in potential nanoparticles and nanotechnology for sensing food-borne pathogens and their toxins in foods and crops: current technologies and limitations. Sens Mat 2014;26:711–36.
[28] Coyle S, Curto VF, Benito-Lopez F, Florea L, Diamond D. Wearable bio and chemical sensors. Wearable sensors. Elsevier; 2014. p. 65–83.
[29] Zhang S, Geryak R, Geldmeier J, Kim S, Tsukruk VV. Synthesis, assembly, and applications of hybrid nanostructures for biosensing. Chem Rev 2017;117:12942–3038.
[30] Luo X, Morrin A, Killard AJ, Smyth MR. Application of nanoparticles in electrochemical sensors and biosensors. Electroanalysis 2006;18:319–26.
[31] Hoseinnejad M, Jafari SM, Katouzian I. Inorganic and metal nanoparticles and their antimicrobial activity in food packaging applications. Crit Rev Microbiol 2018;44:161–81.
[32] Zeng S, Baillargeat D, Ho H-P, Yong K-T. Nanomaterials enhanced surface plasmon resonance for biological and chemical sensing applications. Chem Soc Rev 2014;43:3426–52.
[33] Choi I, Choi Y. Plasmonic nanosensors: review and prospect. IEEE J Select Top Quant Electron 2011;18:1110–21.
[34] Dargahi A, Golestanifar H, Darvishi P, Karami A, Hasan SH, Poormohammadi A, et al. An investigation and comparison of removing heavy metals (lead and chromium) from aqueous solutions using magnesium oxide nanoparticles. Pol J Environ Stud 2016;25:557–62.
[35] Dizaj SM, Lotfipour F, Barzegar-Jalali M, Zarrintan MH, Adibkia K. Antimicrobial activity of the metals and metal oxide nanoparticles. Mater Sci Eng C 2014;44:278–84.
[36] Falcaro P, Ricco R, Yazdi A, Imaz I, Furukawa S, Maspoch D, et al. Application of metal and metal oxide nanoparticles@ MOFs. Coord Chem Rev 2016;307:237–54.
[37] Gautier J, Allard-Vannier E, Munnier E, Soucé M, Chourpa I. Recent advances in theranostic nanocarriers of doxorubicin based on iron oxide and gold nanoparticles. J Control Release 2013;169:48–61.
[38] Osaka T, Matsunaga T, Nakanishi T, Arakaki A, Niwa D, Iida H. Synthesis of magnetic nanoparticles and their application to bioassays. Anal Bioanal Chem 2006;384:593–600.
[39] Alam S, Ahmad R, Pranaw K, Mishra P, Khare SK. Asparaginase conjugated magnetic nanoparticles used for reducing acrylamide formation in food model system. Bioresour Technol 2018;269:121–6.
[40] Christopher FC, Anbalagan S, Kumar PS, Pannerselvam SR, Vaidyanathan VK. Surface adsorption of poisonous Pb (II) ions from water using chitosan functionalised magnetic nanoparticles. IET Nanobiotechnol 2016;11:433–42.
[41] Dey C, Baishya K, Ghosh A, Goswami MM, Ghosh A, Mandal K. Improvement of drug delivery by hyperthermia treatment using magnetic cubic cobalt ferrite nanoparticles. J Magnet Magnet Mater 2017;427:168–74.
[42] Tietze R, Zaloga J, Unterweger H, Lyer S, Friedrich RP, Janko C, et al. Magnetic nanoparticle-based drug delivery for cancer therapy. Biochem Biophys Res Commun 2015;468:463–70.
[43] Masud MK, Na J, Younus M, Hossain MSA, Bando Y, Shiddiky MJ, et al. Superparamagnetic nanoarchitectures for disease-specific biomarker detection. Chem Soc Rev 2019;48:5717–51.
[44] Cao M, Li Z, Wang J, Ge W, Yue T, Li R, et al. Food related applications of magnetic iron oxide nanoparticles: enzyme immobilization, protein purification, and food analysis. Trends Food Sci Technol 2012;27:47–56.
[45] Lee D, Lee J, Kim Y-P, Kim J, Hyeon T, Kim H-S. Highly sensitive and magnetically switchable biosensors using ordered mesoporous carbons. ACS Publications; 2008.
[46] Plouffe BD, Murthy SK, Lewis LH. Fundamentals and application of magnetic particles in cell isolation and enrichment: a review. Rep Prog Phys 2014;78:016601.
[47] Do J, Ahn CH. A polymer lab-on-a-chip for magnetic immunoassay with on-chip sampling and detection capabilities. Lab Chip 2008;8:542–9.

[48] Gao R, Cheng Z, de Mello AJ, Choo J. Wash-free magnetic immunoassay of the PSA cancer marker using SERS and droplet microfluidics. Lab Chip 2016;16:1022–9.
[49] Krishnan S, Goud KY. Magnetic particle bioconjugates: a versatile sensor approach. Magnetochemistry 2019;5:64.
[50] Gan N, Zhou J, Xiong P, Hu F, Cao Y, Li T, et al. An ultrasensitive electrochemiluminescent immunoassay for Aflatoxin M1 in milk, based on extraction by magnetic graphene and detection by antibody-labeled CdTe quantumn dots-carbon nanotubes nanocomposite. Toxins 2013;5:865–83.
[51] Jayasinghe GTM, Domínguez-González R, Bermejo-Barrera P, Moreda-Piñeiro A. Room temperature phosphorescent determination of aflatoxins in fish feed based on molecularly imprinted polymer-Mn-doped ZnS quantum dots. Anal Chim Acta 2020;1103:183–91.
[52] Liu L, Huang Q, Tanveer ZI, Jiang K, Zhang J, Pan H, et al. "Turn off-on" fluorescent sensor based on quantum dots and self-assembled porphyrin for rapid detection of ochratoxin A. Sens Actuators B 2020;302:127212.
[53] Lu Z, Chen X, Hu W. A fluorescence aptasensor based on semiconductor quantum dots and MoS2 nanosheets for ochratoxin A detection. Sens Actuators B 2017; 246:61–7.
[54] Xu H, Yang X, Li G, Zhao C, Liao X. Green synthesis of fluorescent carbon dots for selective detection of tartrazine in food samples. J Agric Food Chem 2015;63: 6707–14.
[55] Wu P, Yan X-P. Doped quantum dots for chemo/biosensing and bioimaging. Chem Soc Rev 2013;42:5489–521.
[56] Azzazy HM, Mansour MM, Kazmierczak SC. From diagnostics to therapy: prospects of quantum dots. Clin Biochem 2007;40:917–27.
[57] He X, Ma N. An overview of recent advances in quantum dots for biomedical applications. Colloids Surf B Biointerfaces 2014;124:118–31.
[58] Joz Majidi H, Mirzaee A, Jafari SM, Amiri M, Shahrousvand M, Babaei A. Fabrication and characterization of graphene oxide-chitosan-zinc oxide ternary nano-hybrids for the corrosion inhibition of mild steel. Int J Biol Macromol 2020;148:1190–200.
[59] Harris PJ. Carbon nanotube composites. Int Mater Rev 2004;49:31–43.
[60] Huang J, Liu Y, You T. Carbon nanofiber based electrochemical biosensors: a review. Anal Methods 2010;2:202–11.
[61] Riehl BL, Riehl BD, King EE, Johnson JM, Schlueter KT. Electrode and sensor having carbon nanostructures. Google Patents; 2011.
[62] Tang H, Chen J, Yao S, Nie L, Kuang Y, Huang Z, et al. Deposition and electrocatalytic properties of platinum on well-aligned carbon nanotube (CNT) arrays for methanol oxidation. Mater Chem Phys 2005;92:548–53.
[63] Llobet E. Gas sensors using carbon nanomaterials: a review. Sens Actuators B 2013; 179:32–45.
[64] Katouzian I, Jafari SM. Protein nanotubes as state-of-the-art nanocarriers: synthesis methods, simulation and applications. J Control Release 2019;303:302–18.
[65] Zaporotskova IV, Boroznina NP, Parkhomenko YN, Kozhitov LV. Carbon nanotubes: sensor properties. A review. Mod Electron Mater 2016;2:95–105.
[66] Schroeder V, Savagatrup S, He M, Lin S, Swager TM. Carbon nanotube chemical sensors. Chem Rev 2018;119:599–663.
[67] Ghodrati M, Mir A, Farmani A. Carbon nanotube field effect transistors–based gas sensors. Nanosensors for smart cities. Elsevier; 2020. p. 171–83.
[68] Bargaoui Y, Troudi M, Bondavalli P, Sghaier N. Gate bias stress effect in single-walled carbon nanotubes field-effect-transistors. Diamond Relat Mater 2018;84: 62–5.
[69] Lee D, Cui T. Low-cost, transparent, and flexible single-walled carbon nanotube nanocomposite based ion-sensitive field-effect transistors for pH/glucose sensing. Biosens Bioelectron 2010;25:2259–64.
[70] Pyo J-Y, Cho W-J. High-sensitivity pH sensor using separative extended-gate field-effect transistors with single-walled carbon-nanotube networks. Jpn J Appl Phys 2018;57:04FP02.
[71] Zeinabad HA, Zarrabian A, Saboury AA, Alizadeh AM, Falahati M. Interaction of single and multi wall carbon nanotubes with the biological systems: tau protein and PC12 cells as targets. Sci Rep 2016;6:26508.
[72] Georgakilas V, Perman JA, Tucek J, Zboril R. Broad family of carbon nanoallotropes: classification, chemistry, and applications of fullerenes, carbon dots, nanotubes, graphene, nanodiamonds, and combined superstructures. Chem Rev 2015;115: 4744–822.
[73] Ritter KA, Lyding JW. The influence of edge structure on the electronic properties of graphene quantum dots and nanoribbons. Nat Mater 2009;8:235–42.
[74] Joz Majidi H, Babaei A, Arab Bafrani Z, Shahrampour D, Zabihi E, Jafari SM. Investigating the best strategy to diminish the toxicity and enhance the antibacterial activity of graphene oxide by chitosan addition. Carbohydr Polym 2019;225:115220.
[75] Bagheri M, Jafari SM, Eikani MH. Development of ternary nanoadsorbent composites of graphene oxide, activated carbon, and zero-valent iron nanoparticles for food applications. Food Sci Nutr 2019;7:2827–35.
[76] Zhang J, Yang H, Shen G, Cheng P, Zhang J, Guo S. Reduction of graphene oxide via L-ascorbic acid. Chem Commun 2010;46:1112–4.
[77] Shen J, Zhu Y, Yang X, Li C. Graphene quantum dots: emergent nanolights for bioimaging, sensors, catalysis and photovoltaic devices. Chem Commun 2012;48: 3686–99.
[78] Chen D, Feng H, Li J. Graphene oxide: preparation, functionalization, and electrochemical applications. Chem Rev 2012;112:6027–53.
[79] Georgakilas V, Otyepka M, Bourlinos AB, Chandra V, Kim N, Kemp KC, et al. Functionalization of graphene: covalent and non-covalent approaches, derivatives and applications. Chem Rev 2012;112:6156–214.
[80] Kuila T, Bose S, Khanra P, Mishra AK, Kim NH, Lee JH. Recent advances in graphene-based biosensors. Biosens Bioelectron 2011;26:4637–48.
[81] Liu Y, Dong X, Chen P. Biological and chemical sensors based on graphene materials. Chem Soc Rev 2012;41:2283–307.
[82] Gupta S, Irihamye A. Probing the nature of electron transfer in metalloproteins on graphene-family materials as nanobiocatalytic scaffold using electrochemistry. AIP Adv 2015;5:037106.
[83] Bharadwaj S, Pandey A, Yagci B, Ozguz V, Qureshi A. Graphene nano-mesh-Ag-ZnO hybrid paper for sensitive SERS sensing and self-cleaning of organic pollutants. Chem Eng J 2018;336:445–55.
[84] Feng S, Dos Santos MC, Carvalho BR, Lv R, Li Q, Fujisawa K, et al. Ultrasensitive molecular sensor using N-doped graphene through enhanced Raman scattering. Sci Adv 2016;2:e1600322.
[85] Meng Y, Yan X, Wang Y. A simple preparation of Ag@ graphene nanocomposites for surface-enhanced Raman spectroscopy of fluorescent anticancer drug. Chem Phys Lett 2016;651:84–7.
[86] Yuan F, Ding L, Li Y, Li X, Fan L, Zhou S, et al. Multicolor fluorescent graphene quantum dots colorimetrically responsive to all-pH and a wide temperature range. Nanoscale 2015;7:11727–33.
[87] Tibbetts GG, Lake ML, Strong KL, Rice BP. A review of the fabrication and properties of vapor-grown carbon nanofiber/polymer composites. Comp Sci Technol 2007;67: 1709–18.
[88] Vamvakaki V, Tsagaraki K, Chaniotakis N. Carbon nanofiber-based glucose biosensor. Anal Chem 2006;78:5538–42.
[89] Rassaei L, Sillanpää M, Bonné MJ, Marken F. Carbon nanofiber–polystyrene composite electrodes for electroanalytical processes. Electroanalysis 2007;19:1461–6.
[90] Kshetri T, Tran DT, Nguyen DC, Kim NH, Lau K-t, Lee JH. Ternary graphene-carbon nanofibers-carbon nanotubes structure for hybrid supercapacitor. Chem Eng J 2020;380:122543.
[91] Lupan O, Postica V, Wolff N, Polonskyi O, Duppel V, Kaidas V, et al. Localized synthesis of iron oxide nanowires and fabrication of high performance nanosensors based on a single Fe2O3 nanowire. Small 2017;13:1602868.
[92] Tonezzer M, Kim J-H, Lee J-H, Iannotta S, Kim SS. Predictive gas sensor based on thermal fingerprints from Pt-SnO2 nanowires. Sens Actuators B 2019;281:670–8.
[93] Huang J, Wan Q. Gas sensors based on semiconducting metal oxide one-dimensional nanostructures. Sensors 2009;9:9903–24.
[94] Zhai T, Yao J. One-dimensional nanostructures. Wiley Online Library; 2013.
[95] Ambhorkar P, Wang Z, Ko H, Lee S, Koo K-i, Kim K, et al. Nanowire-based biosensors: from growth to applications. Micromachines 2018;9:679.
[96] Zhang A, Zheng G, Lieber CM. Nanowire field-effect transistor sensors. Nanowires. Springer; 2016. p. 255–75.
[97] Ramgir NS, Yang Y, Zacharias M. Nanowire-based sensors. Small 2010;6:1705–22.
[98] Wanekaya AK, Chen W, Myung NV, Mulchandani A. Nanowire-based electrochemical biosensors. Electroanalysis 2006;18:533–50.
[99] Kitikul J, Satienperakul S, Preechaworapun A, Pookmanee P, Tangkuaram T. A simple flow amperometric electrochemical biosensor based on chitosan scaffolds and gold nanowires modified on a glassy carbon electrode for detection of glutamate in food products. Electroanalysis 2017;29:264–71.
[100] Nikoleli G-P. Advanced lipid based biosensors for food analysis. Advances in food and nutrition research. Elsevier; 2020. p. 301–21.
[101] Alehosseini E, Jafari SM. Micro/nano-encapsulated phase change materials (PCMs) as emerging materials for the food industry. Trends Food Sci Technol 2019;91: 116–28.
[102] Feng C, Khulbe K, Matsuura T. Recent progress in the preparation, characterization, and applications of nanofibers and nanofiber membranes via electrospinning/interfacial polymerization. J Appl Polym Sci 2010;115:756–76.
[103] Yokoyama Y, Hattori S, Yoshikawa C, Yasuda Y, Koyama H, Takato T, et al. Novel wet electrospinning system for fabrication of spongiform nanofiber 3-dimensional fabric. Mater Lett 2009;63:754–6.
[104] Ohzawa Y, Nagano Y, Matsuo T. Studies on dry spinning. I. Fundamental equations. J Appl Polym Sci 1969;13:257–83.
[105] Hutmacher DW, Dalton PD. Melt electrospinning. Chem Asian J 2011;6:44–56.
[106] Wyatt TP, Chien AT, Kumar S, Yao D. Development of a gel spinning process for high-strength poly (ethylene oxide) fibers. Polym Eng Sci 2014;54:2839–47.
[107] Hoseyni SZ, Jafari SM, Shahiri Tabarestani H, Ghorbani M, Assadpour E, Sabaghi M. Production and characterization of catechin-loaded electrospun nanofibers from Azivash gum- polyvinyl alcohol. Carbohydr Polym 2020;235:115979.
[108] Rostami M, Yousefi M, Khezerlou A, Aman Mohammadi M, Jafari SM. Application of different biopolymers for nanoencapsulation of antioxidants via electrohydrodynamic processes. Food Hydrocoll 2019;97:105170.
[109] Khoshnoudi-Nia S, Sharif N, Jafari SM. Loading of phenolic compounds into electrospun nanofibers and electrosprayed nanoparticles. Trends Food Sci Technol 2020;95:59–74.
[110] Mazoochi T, Hamadanian M, Ahmadi M, Jabbari V. Investigation on the morphological characteristics of nanofiberous membrane as electrospun in the different processing parameters. Int J Industr Chem 2012;3:2.
[111] Rezaei A, Fathi M, Jafari SM. Nanoencapsulation of hydrophobic and low-soluble food bioactive compounds within different nanocarriers. Food Hydrocoll 2019; 88:146–62.
[112] Soleimanifar M, Jafari SM, Assadpour E. Encapsulation of olive leaf phenolics within electrosprayed whey protein nanoparticles; production and characterization. Food Hydrocoll 2020;101:105572.
[113] Xue J, Wu T, Dai Y, Xia Y. Electrospinning and electrospun nanofibers: methods, materials, and applications. Chem Rev 2019;119:5298–415.
[114] Shaibani PM, Jiang K, Haghighat G, Hassanpourfard M, Etayash H, Naicker S, et al. The detection of Escherichia coli (E. coli) with the pH sensitive hydrogel nanofiber-light addressable potentiometric sensor (NF-LAPS). Sens Actuators B 2016;226:176–83.

[115] Shaibani PM, Etayash H, Jiang K, Sohrabi A, Hassanpourfard M, Naicker S, et al. Portable nanofiber-light addressable potentiometric sensor for rapid Escherichia coli detection in orange juice. ACS Sensors 2018;3:815–22.
[116] Karuppuswami S, Matta LL, Alocilja EC, Chahal P. A wireless RFID compatible sensor tag using gold nanoparticle markers for pathogen detection in the liquid food supply chain. IEEE Sensors Lett 2018;2:1–4.
[117] Li H, Ahmad W, Rong Y, Chen Q, Zuo M, Ouyang Q, et al. Designing an aptamer based magnetic and upconversion nanoparticles conjugated fluorescence sensor for screening Escherichia coli in food. Food Control 2020;107:106761.
[118] Xu Y, Dai Y, Li C, Zhang H, Guo M, Yang Y. PC software-based portable cyclic voltammetry system with PB-MCNT-GNPs-modified electrodes for E. coli detection. Rev Sci Instrum 2020;91:014103.
[119] Du J, Wu S, Niu L, Li J, Zhao D, Bai Y. A gold nanoparticles-assisted multiplex PCR assay for simultaneous detection of Salmonella typhimurium, Listeria monocytogenes and Escherichia coli O157: H7. Anal Methods 2020;12:212–7.
[120] Chen Z-g, Zhong H-x, Luo H, Zhang R-y, Huang J-r. Recombinase polymerase amplification combined with unmodified gold nanoparticles for Salmonella detection in milk. Food Anal Methods 2019;12:190–7.
[121] Yi J, Wu P, Li G, Xiao W, Li L, He Y, et al. A composite prepared from carboxymethyl chitosan and aptamer-modified gold nanoparticles for the colorimetric determination of Salmonella typhimurium. Microchim Acta 2019;186:711.
[122] Appaturi JN, Pulingam T, Thong KL, Muniandy S, Ahmad N, Leo BF. Rapid and sensitive detection of Salmonella with reduced graphene oxide-carbon nanotube based electrochemical aptasensor. Anal Biochem 2020;589:113489.
[123] Abbaspour A, Norouz-Sarvestani F, Noori A, Soltani N. Aptamer-conjugated silver nanoparticles for electrochemical dual-aptamer-based sandwich detection of staphylococcus aureus. Biosens Bioelectron 2015;68:149–55.
[124] Bhardwaj J, Devarakonda S, Kumar S, Jang J. Development of a paper-based electrochemical immunosensor using an antibody-single walled carbon nanotubes bioconjugate modified electrode for label-free detection of foodborne pathogens. Sens Actuators B 2017;253:115–23.
[125] Mathur A, Gupta R, Kondal S, Wadhwa S, Pudake RN, Kansal R, et al. A new tactics for the detection of S. aureus via paper based geno-interface incorporated with graphene nano dots and zeolites. Int J Biol Macromol 2018;112:364–70.
[126] Yin M, Wu C, Li H, Jia Z, Deng Q, Wang S, et al. Simultaneous sensing of seven pathogenic bacteria by guanidine-functionalized upconversion fluorescent nanoparticles. ACS Omega 2019;4:8953–9.
[127] Wang H, Xiu Y, Chen Y, Sun L, Yang L, Chen H, et al. Electrochemical immunosensor based on an antibody-hierarchical mesoporous SiO 2 for the detection of Staphylococcus aureus. RSC Adv 2019;9:16278–87.
[128] Rodríguez-Lorenzo L, Garrido-Maestu A, Bhunia AK, Espiña B, Prado M, Diéguez L, et al. Gold nanostars for the detection of foodborne pathogens via surface-enhanced Raman scattering combined with microfluidics. ACS Appl Nano Mater 2019;2:6081–6.
[129] Teixeira A, Paris JL, Roumani F, Diéguez L, Prado M, Espiña B, et al. Multifuntional gold nanoparticles for the SERS detection of pathogens combined with a LAMP–in–microdroplets approach. Materials 2020;13:1934.
[130] Xiang Y, Camarada MB, Wen Y, Wu H, Chen J, Li M, et al. Simple voltammetric analyses of ochratoxin A in food samples using highly-stable and anti-fouling black phosphorene nanosensor. Electrochim Acta 2018;282:490–8.
[131] Shao B, Ma X, Zhao S, Lv Y, Hun X, Wang H, et al. Nanogapped Au (core)@ Au-Ag (shell) structures coupled with Fe3O4 magnetic nanoparticles for the detection of Ochratoxin A. Anal Chim Acta 2018;1033:165–72.
[132] Lv L, Cui C, Liang C, Quan W, Wang S, Guo Z. Aptamer-based single-walled carbon nanohorn sensors for ochratoxin A detection. Food Control 2016;60:296–301.
[133] Devarayan K, Kim B-S. Reversible and universal pH sensing cellulose nanofibers for health monitor. Sens Actuators B 2015;209:281–6.
[134] Aghaei Z, Emadzadeh B, Ghorani B, Kadkhodaee R. Cellulose acetate nanofibres containing alizarin as a halochromic sensor for the qualitative assessment of rainbow trout fish spoilage. Food Bioproc Tech 2018;11:1087–95.
[135] Aghaei Z, Ghorani B, Emadzadeh B, Kadkhodaee R, Tucker N. Protein-based halochromic electrospun nanosensor for monitoring trout fish freshness. Food Control 2020;111:107065.
[136] Sanger A, Kumar A, Kumar A, Chandra R. Highly sensitive and selective hydrogen gas sensor using sputtered grown Pd decorated MnO2 nanowalls. Sens Actuators B 2016;234:8–14.
[137] Liu SF, Petty AR, Sazama GT, Swager TM. Single-walled carbon nanotube/metalloporphyrin composites for the chemiresistive detection of amines and meat spoilage. Angew Chem Int Ed 2015;54:6554–7.
[138] Heli B, Morales-Narváez E, Golmohammadi H, Ajji A, Merkoçi A. Modulation of population density and size of silver nanoparticles embedded in bacterial cellulose via ammonia exposure: visual detection of volatile compounds in a piece of plasmonic nanopaper. Nanoscale 2016;8:7984–91.
[139] Valdez M, Gupta SK, Lozano K, Mao Y. ForceSpun polydiacetylene nanofibers as colorimetric sensor for food spoilage detection. Sens Actuators B 2019;297:126734.
[140] Tanguy NR, Wiltshire B, Arjmand M, Zarifi MH, Yan N. Highly sensitive and contactless ammonia detection based on nanocomposites of phosphate-functionalized reduced graphene oxide/polyaniline immobilized on microstrip resonators. ACS Appl Mater Interfaces 2020;12:9746–54.
[141] Ertas N, Gonulalan Z, Yildirim Y, Kum E. Detection of Staphylococcus aureus enterotoxins in sheep cheese and dairy desserts by multiplex PCR technique. Int J Food Microbiol 2010;142:74–7.
[142] Azinheiro S, Kant K, Shahbazi M-A, Garrido-Maestu A, Prado M, Dieguez L. A smart microfluidic platform for rapid multiplexed detection of foodborne pathogens. Food Control 2020:107242.
[143] Jahn I, Žukovskaja O, Zheng X-S, Weber K, Bocklitz T, Cialla-May D, et al. Surface-enhanced Raman spectroscopy and microfluidic platforms: challenges, solutions and potential applications. Analyst 2017;142:1022–47.
[144] Eivazzadeh-Keihan R, Pashazadeh P, Hejazi M, de la Guardia M, Mokhtarzadeh A. Recent advances in nanomaterial-mediated bio and immune sensors for detection of aflatoxin in food products. TrAC Trends Anal Chem 2017;87:112–28.
[145] Paniel N, Radoi A, Marty J-L. Development of an electrochemical biosensor for the detection of aflatoxin M1 in milk. Sensors 2010;10:9439–48.
[146] Bento J, Pena A, Lino C, Pereira J. Determination of ochratoxin A content in wheat bread samples collected from the Algarve and Bragança regions, Portugal: winter 2007. Microchem J 2009;91:165–9.
[147] Dhahri R, Hjiri M, El Mir L, Bonavita A, Iannazzo D, Latino M, et al. Gas sensing properties of Al-doped ZnO for UV-activated CO detection. J Phys D Appl Phys 2016;49:135502.
[148] Peter A, Mihaly-Cozmuta A, Mihaly-Cozmuta L, Nicula C. Nanosensor based on TiO2 for detection of oxygen in damaged vacuum packages. Carpathian J Food Sci Technol 2013;5:9–12.
[149] Amin K, Hameid II HA, Elsttar AA. Effect of food azo dyes tartrazine and carmoisine on biochemical parameters related to renal, hepatic function and oxidative stress biomarkers in young male rats. Food Chem Toxicol 2010;48:2994–9.
[150] Nambiar AP, Sanyal M, Shrivastav PS. Simultaneous densitometric determination of eight food colors and four sweeteners in candies, jellies, beverages and pharmaceuticals by normal-phase high performance thin-layer chromatography using a single elution protocol. J Chromatogr A 2018;1572:152–61.
[151] Yilmaz UT, Ergun F, Yilmaz H. Determination of the food dye carmine in milk and candy products by differential pulse polarography. J Food Drug Analysis 2014;22:329–35.
[152] Gómez M, Arancibia V, Aliaga M, Núñez C, Rojas-Romo C. Determination of Sudan I in drinks containing Sunset yellow by adsorptive stripping voltammetry. Food Chem 2016;212:807–13.
[153] Le THH, Nguyen TQH, Tran CS, Vu TT, Nguyen TL, Ta TT, et al. Screening determination of food additives using capillary electrophoresis coupled with contactless conductivity detection: a case study in Vietnam. Food Control 2017;77:281–9.
[154] Ma M, Luo X, Chen B, Su S, Yao S. Simultaneous determination of water-soluble and fat-soluble synthetic colorants in foodstuff by high-performance liquid chromatography–diode array detection–electrospray mass spectrometry. J Chromatogr A 2006;1103:170–6.
[155] Cerón-García M, González-López C, Camacho-Rodríguez J, López-Rosales L, García-Camacho F, Molina-Grima E. Maximizing carotenoid extraction from microalgae used as food additives and determined by liquid chromatography (HPLC). Food Chem 2018;257:316–24.
[156] Pressman P, Clemens R, Hayes W, Reddy C. Food additive safety: a review of toxicologic and regulatory issues. Toxicol Res Appl 2017;1 (2397847317723572).
[157] Mahdavi SA, Jafari SM, Ghorbani M, Assadpoor E. Spray-drying microencapsulation of anthocyanins by natural biopolymers: a review. Drying Technol 2014;32:509–18.
[158] Alves SP, Brum DM, de Andrade ECB, Netto ADP. Determination of synthetic dyes in selected foodstuffs by high performance liquid chromatography with UV-DAD detection. Food Chem 2008;107:489–96.
[159] Hassan G. Effects of some synthetic coloring additives on DNA damage and chromosomal aberrations of rats. Arab J Biotech 2010;13:13–24.
[160] Yin H, Zhou Y, Meng X, Tang T, Ai S, Zhu L. Electrochemical behaviour of Sudan I at Fe3O4 nanoparticles modified glassy carbon electrode and its determination in food samples. Food Chem 2011;127:1348–53.
[161] Palanisamy S, Thangavelu K, Chen S-M, Thirumalraj B, Liu X-H. Preparation and characterization of gold nanoparticles decorated on graphene oxide@polydopamine composite: application for sensitive and low potential detection of catechol. Sens Actuators B 2016;233:298–306.
[162] Palanisamy S, Sakthinathan S, Chen S-M, Thirumalraj B, Wu T-H, Lou B-S, et al. Preparation of β-cyclodextrin entrapped graphite composite for sensitive detection of dopamine. Carbohydr Polym 2016;135:267–73.
[163] Zhang L, Zhang X, Li X, Peng Y, Shen H, Zhang Y. Determination of Sudan I using electrochemically reduced graphene oxide. Analytic Lett 2013;46:923–35.
[164] Palanisamy S, Kokulnathan T, Chen S-M, Velusamy V, Ramaraj SK. Voltammetric determination of Sudan I in food samples based on platinum nanoparticles decorated on graphene-β-cyclodextrin modified electrode. J Electroanal Chem 2017;794:64–70.
[165] Mahmoudi-Moghaddam H, Tajik S, Beitollahi H. Highly sensitive electrochemical sensor based on La3+-doped Co3O4 nanocubes for determination of sudan I content in food samples. Food Chem 2019;286:191–6.
[166] Tajik S, Aflatoonian MR, Shabanzade R, Beitollahi H, Alizadeh R. Amplified electrochemical sensor employing ZnO-CuO nanoplates for sensitive analysis of Sudan I. Int J Environ Anal Chem 2020;100:109–20.
[167] Vinothkumar V, Sangili A, Chen S-M, Chen T-W, Abinaya M, Sethupathi V. Voltammetric determination of Sudan I by using Bi2WO6 nanosheets modified glassy carbon electrode. Int J Electrochem Sci 2020;15:2414–29.
[168] Yang YJ, Li W. CTAB functionalized graphene oxide/multiwalled carbon nanotube composite modified electrode for the simultaneous determination of sunset yellow and tartrazine. Russian J Electrochem 2015;51:218–26.
[169] Li J, Wang X, Duan H, Wang Y, Bu Y, Luo C. Based on magnetic graphene oxide highly sensitive and selective imprinted sensor for determination of sunset yellow. Talanta 2016;147:169–76.
[170] Tahtaisleyen S, Gorduk O, Sahin Y. Electrochemical determination of tartrazine using a Graphene/Poly (L-Phenylalanine) modified pencil graphite electrode. Analytic Lett 2020:1–21.

[171] Kolozof P-A, Florou AB, Spyrou K, Hrbac J, Prodromidis MI. In-situ tailoring of the electrocatalytic properties of screen-printed graphite electrodes with sparked generated molybdenum nanoparticles for the simultaneous voltammetric determination of sunset yellow and tartrazine. Sens Actuators B 2020;304:127268.
[172] Yücebaş BB, Yaman YT, Bolat G, Özgür E, Uzun L, Abaci S. Molecular imprinted polymer based electrochemical sensor for selective detection of paraben. Sens Actuators B 2020;305:127368.
[173] Gao T, Cao X, Ge P, Dong J, Yang S, Xu H, et al. A self-assembled fluorescent organic nanoprobe and its application for sulfite detection in food samples and living systems. Org Biomol Chem 2017;15:4375–82.
[174] Fitriyana F, Kurniawan F. Polyaniline-invertase-gold nanoparticles modified gold electrode for sucrose detection. Indian J Chem 2015;15:226–33.
[175] Bagal-Kestwal DR, Chiang B-H. Platinum nanoparticle-carbon nanotubes dispersed in gum Arabic-corn flour composite-enzymes for an electrochemical sucrose sensing in commercial juice. Ionics 2019:1–14.
[176] Li Y, Hodak M, Lu W, Bernholc J. Selective sensing of ethylene and glucose using carbon-nanotube-based sensors: an ab initio investigation. Nanoscale 2017;9:1687–98.
[177] Kumar N, Seth R, Kumar H. Colorimetric detection of melamine in milk by citrate-stabilized gold nanoparticles. Anal Biochem 2014;456:43–9.
[178] Kuang H, Chen W, Yan W, Xu L, Zhu Y, Liu L, et al. Crown ether assembly of gold nanoparticles: melamine sensor. Biosens Bioelectron 2011;26:2032–7.
[179] Ai K, Liu Y, Lu L. Hydrogen-bonding recognition-induced color change of gold nanoparticles for visual detection of melamine in raw milk and infant formula. J Am Chem Soc 2009;131:9496–7.
[180] Du J, Wang Y, Zhang W. Gold nanoparticles-based chemiluminescence resonance energy transfer for ultrasensitive detection of melamine. Spectrochim Acta A Mol Biomol Spectrosc 2015;149:698–702.
[181] Ping H, Zhang M, Li H, Li S, Chen Q, Sun C, et al. Visual detection of melamine in raw milk by label-free silver nanoparticles. Food Control 2012;23:191–7.
[182] Bittar DB, Catelani TA, Nigoghossian K, Barud HDS, Ribeiro SJL, Pezza L, et al. Optimized synthesis of silver nanoparticles by factorial design with application for the determination of melamine in milk. Analytic Lett 2017;50:829–41.
[183] Kumar N, Kumar H, Mann B, Seth R. Colorimetric determination of melamine in milk using unmodified silver nanoparticles. Spectrochim Acta A Mol Biomol Spectrosc 2016;156:89–97.
[184] Varun S, Daniel SK, Gorthi SS. Rapid sensing of melamine in milk by interference green synthesis of silver nanoparticles. Mater Sci Eng C 2017;74:253–8.
[185] Borase HP, Patil CD, Salunkhe RB, Suryawanshi RK, Salunke BK, Patil SV. Biofunctionalized silver nanoparticles as a novel colorimetric probe for melamine detection in raw milk. Biotechnol Appl Biochem 2015;62:652–62.
[186] Daniel SK, Julius LAN, Gorthi SS. Instantaneous detection of melamine by interference biosynthesis of silver nanoparticles. Sens Actuators B 2017;238:641–50.
[187] Kumar TV, Sundramoorthy AK. Non-enzymatic electrochemical detection of urea on silver nanoparticles anchored nitrogen-doped single-walled carbon nanotube modified electrode. J Electrochem Soc 2018;165:B3006.
[188] Kumar V, Chopra A, Arora S, Yadav S, Kumar S, Kaur I. Amperometric sensing of urea using edge activated graphene nanoplatelets. RSC Adv 2015;5:13278–84.
[189] Kumar V, Kaur I, Arora S, Mehla R, Vellingiri K, Kim K-H. Graphene nanoplatelet/graphitized nanodiamond-based nanocomposite for mediator-free electrochemical sensing of urea. Food Chem 2020;303:125375.
[190] Migliorini FL, Sanfelice RC, Mercante LA, Andre RS, Mattoso LH, Correa DS. Urea impedimetric biosensing using electrospun nanofibers modified with zinc oxide nanoparticles. Appl Surf Sci 2018;443:18–23.
[191] Bahrami A, Delshadi R, Jafari SM, Williams L. Nanoencapsulated nisin: an engineered natural antimicrobial system for the food industry. Trends Food Sci Technol 2019;94:20–31.
[192] Brown CA, Jeong K-S, Poppenga RH, Puschner B, Miller DM, Ellis AE, et al. Outbreaks of renal failure associated with melamine and cyanuric acid in dogs and cats in 2004 and 2007. J Vet Diagn Invest 2007;19:525–31.
[193] Xiu C, Klein K. Melamine in milk products in China: examining the factors that led to deliberate use of the contaminant. Food Policy 2010;35:463–70.
[194] Ibrahim AA, Ahmad R, Umar A, Al-Assiri M, Al-Salami A, Kumar R, et al. Two-dimensional ytterbium oxide nanodisks based biosensor for selective detection of urea. Biosens Bioelectron 2017;98:254–60.
[195] Kaushik A, Solanki PR, Ansari AA, Sumana G, Ahmad S, Malhotra BD. Iron oxide-chitosan nanobiocomposite for urea sensor. Sens Actuators B 2009;138:572–80.
[196] Solanki PR, Kaushik A, Ansari AA, Sumana G, Malhotra B. Zinc oxide-chitosan nanobiocomposite for urea sensor. Appl Phys Lett 2008;93:163903.
[197] Tak M, Gupta V, Tomar M. Zinc oxide–multiwalled carbon nanotubes hybrid nanocomposite based urea biosensor. J Mater Chem B 2013;1:6392–401.
[198] Velychko T, Soldatkin O, Melnyk V, Marchenko S, Kirdeciler S, Akata B, et al. A novel conductometric urea biosensor with improved analytical characteristic based on recombinant urease adsorbed on nanoparticle of silicalite. Nanoscale Res Lett 2016;11:106.